

Astrophysical Inputs to Atmospheric Neutrinos

1. cosmic ray spectra and composition
2. uncertainties and their impact on atmospheric neutrino flux
3. Astrophysical neutrinos and outlook

based on Garzelli, Moch, Sigl, JHEP 10 (2015) 115



Günter Sigl

II. Institut theoretische Physik, Universität Hamburg

Calculation of Atmospheric Lepton Fluxes

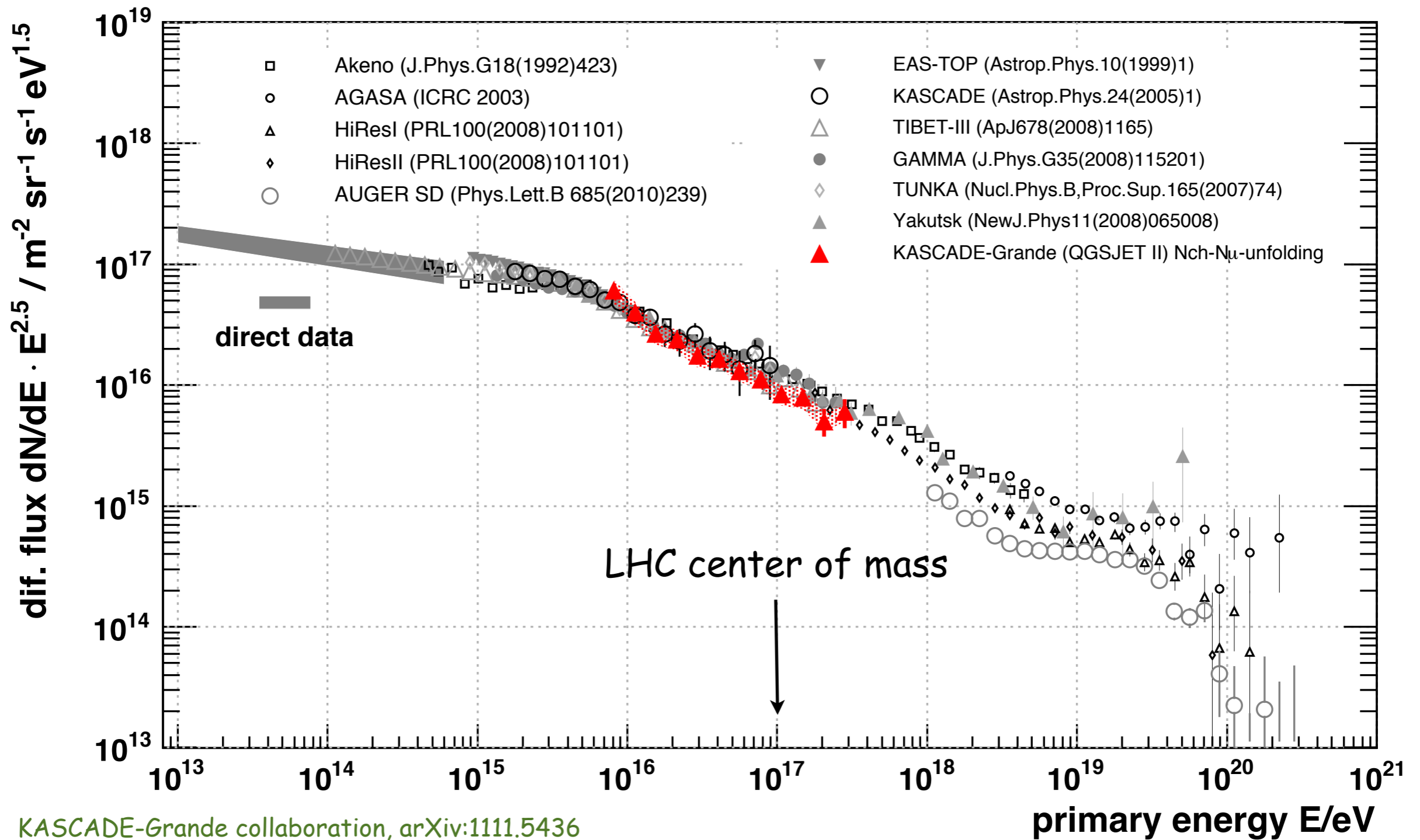
$$\frac{d\phi_j}{dX} = -\frac{\phi_j}{\lambda_{j,int}} - \frac{\phi_j}{\lambda_{j,dec}} + \sum_{k \neq j} S_{\text{prod}}(k \rightarrow j) + \sum_{k \neq j} S_{\text{decay}}(k \rightarrow j) + S_{\text{reg}}(j \rightarrow j).$$

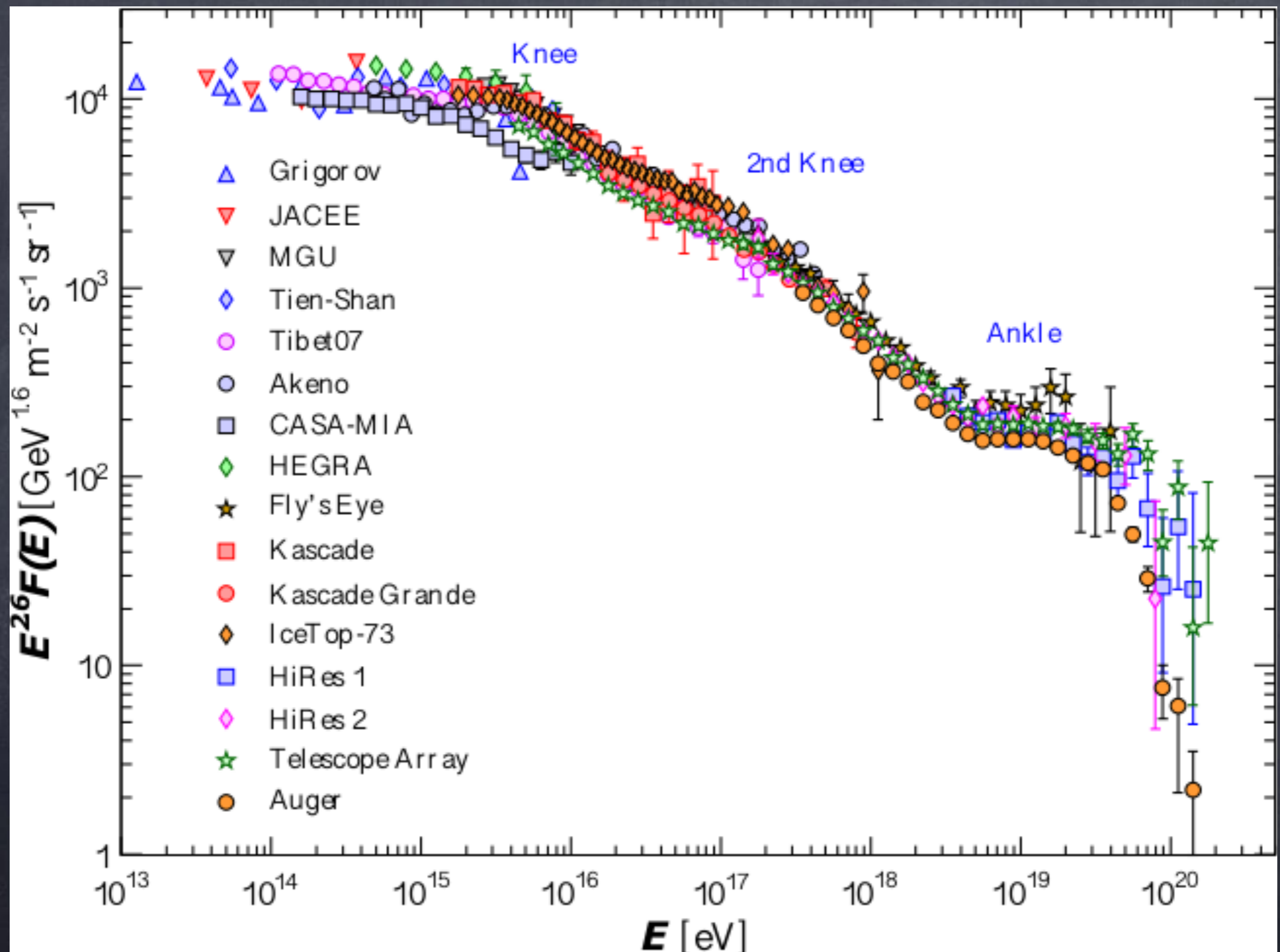
There is a critical energy above which interactions dominate over decay; for charged pions it is about 20 GeV, for charmed mesons it is much higher, $\sim 10^7$ GeV

$$S_{\text{prod}}(k \rightarrow j) = \int_{E_j}^{\infty} dE_k \frac{\phi_k(E_k, X)}{\lambda_k(E_k)} \frac{1}{\sigma_k} \frac{d\sigma_{k \rightarrow j}(E_k, E_j)}{dE_j} \sim \frac{\phi_k(E_j, X)}{\lambda_k(E_j)} Z_{kj}(E_j),$$
$$S_{\text{decay}}(j \rightarrow l) = \int_{E_l}^{\infty} dE_j \frac{\phi_j(E_j, X)}{\lambda_j(E_j)} \frac{1}{\Gamma_j} \frac{d\Gamma_{j \rightarrow l}(E_j, E_l)}{dE_l} \sim \frac{\phi_j(E_l, X)}{\lambda_j(E_l)} Z_{jl}(E_l).$$

Most relevant for us is the all-nucleon flux which depends both on the all-particle flux and the mass composition

The All Particle Cosmic Ray Spectrum

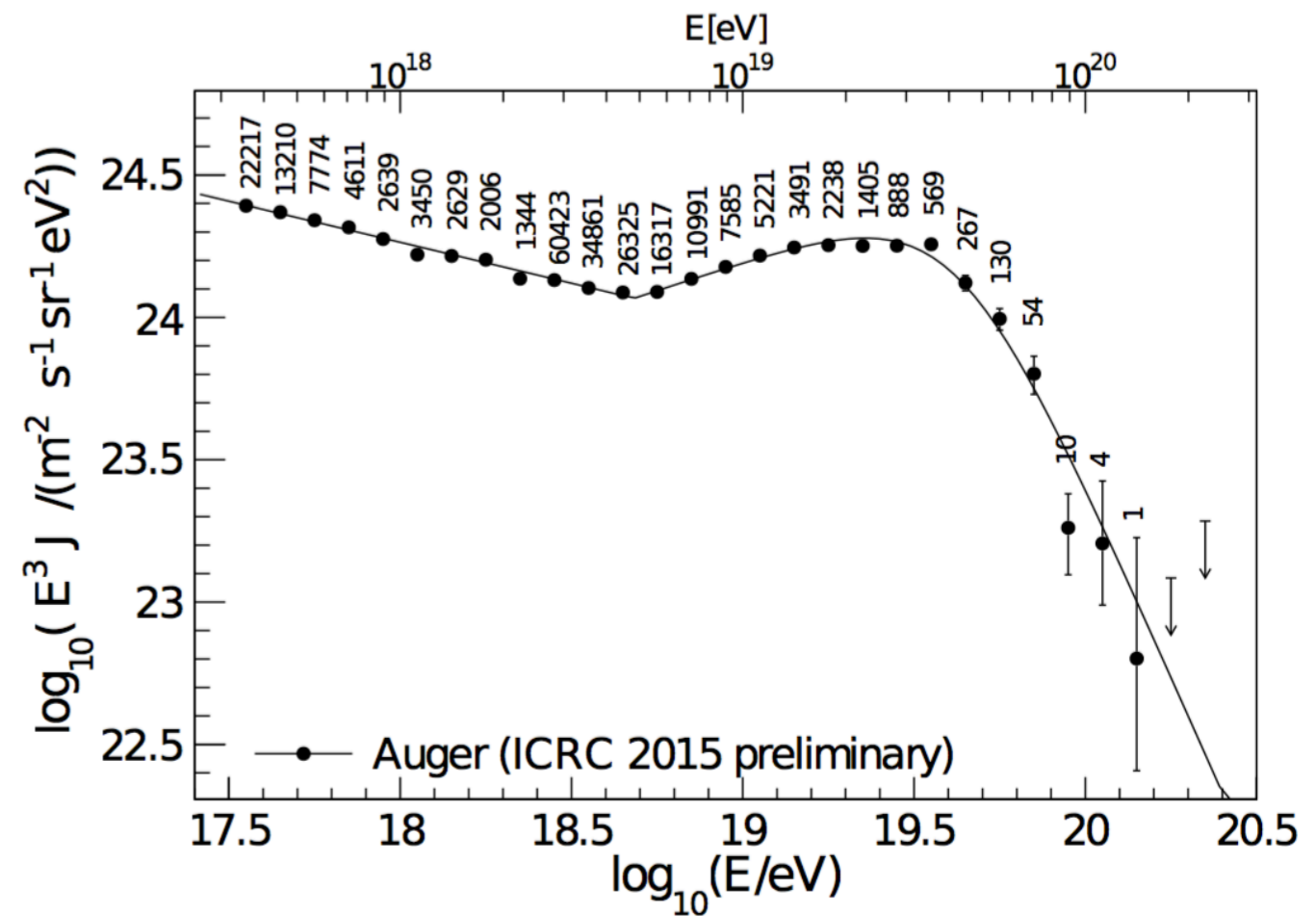
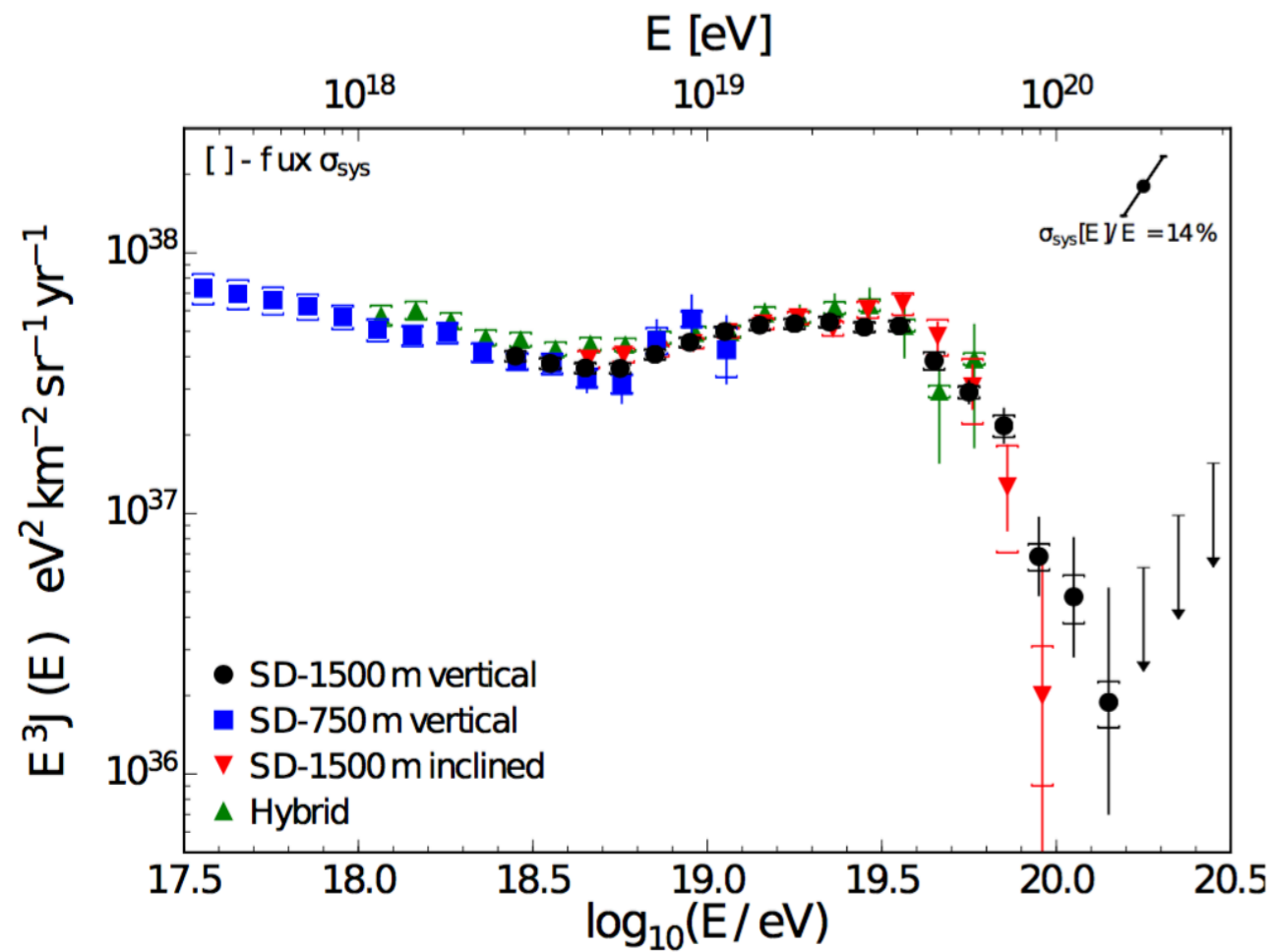




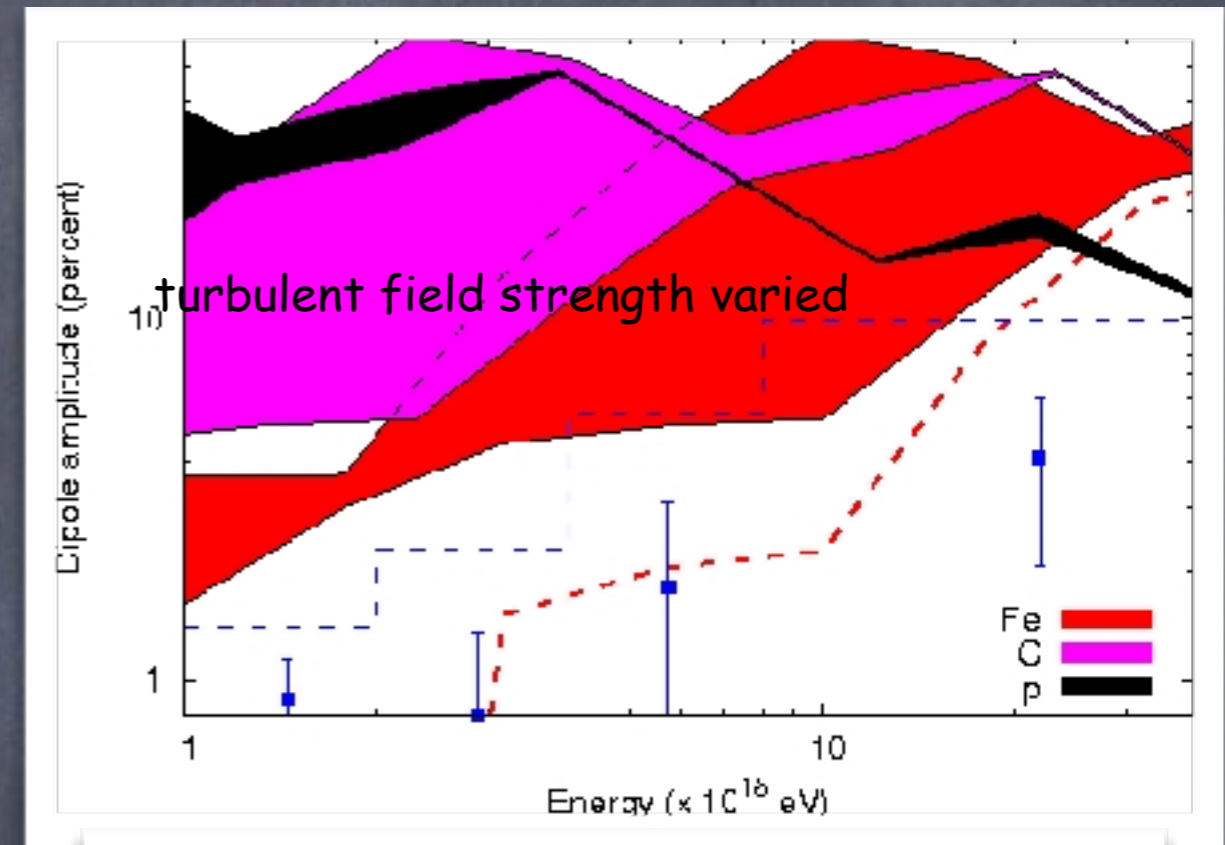
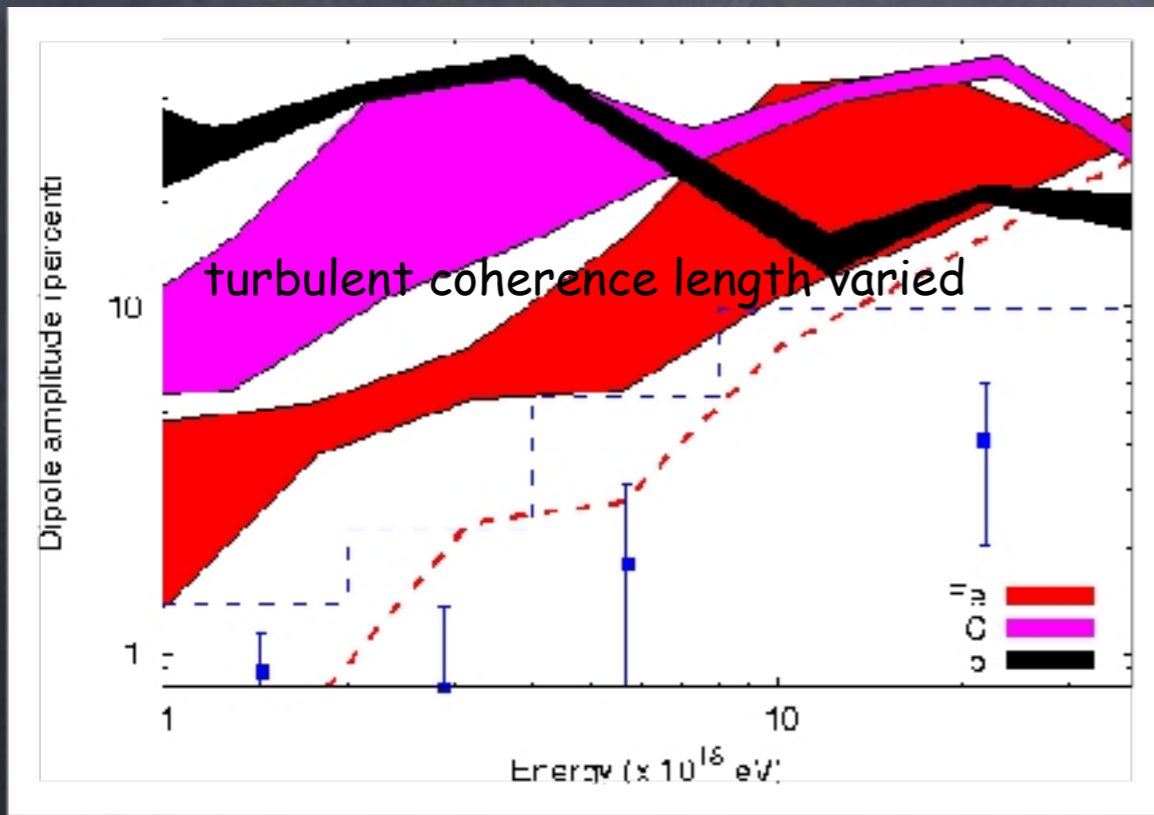
Pierre Auger Spectra

Auger exposure = 50000 km² sr yr, 102901 events above 3x10¹⁸ eV until end 2014

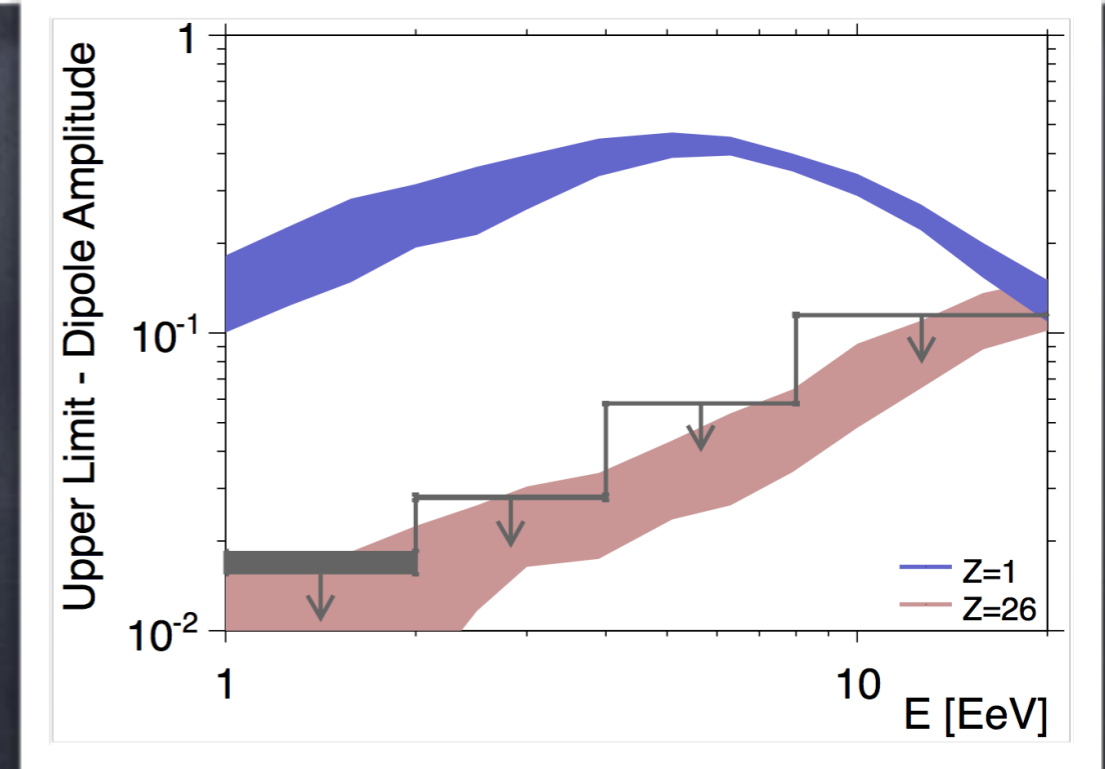
Pierre Auger Collaboration, PRL 101, 061101 (2008)
and Phys.Lett.B 685 (2010) 239
ICRC 2015, arXiv:1509.03732



Composition and the Transition Galactic/Extragalactic Cosmic Rays



Giacinti, Kachelriess, Semikoz, Sigl,
 JCAP 07 (2012) 031
 and Pierre Auger Collaboration, Astrophys.J. 762 (2012) L13



KASCADE data suggest a heavy composition below $\sim 10^{18}$ eV possibly becoming lighter around 10^{18} eV

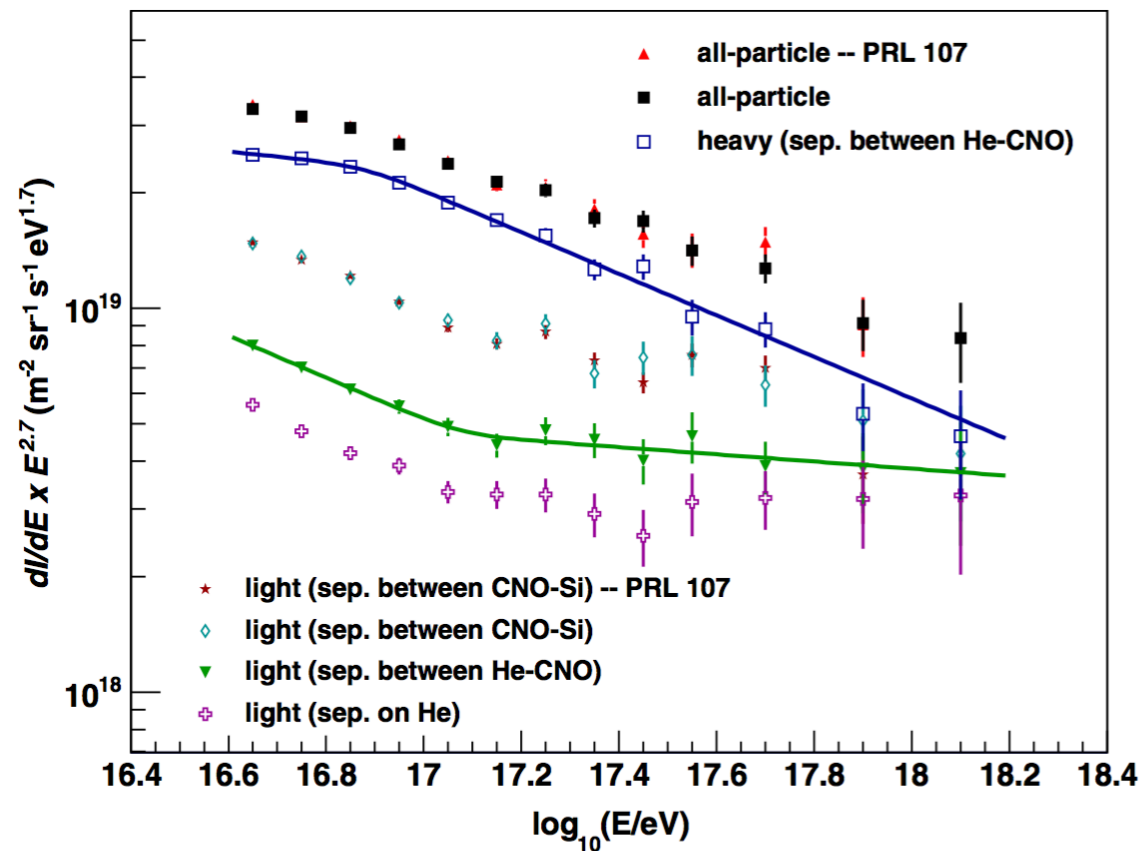
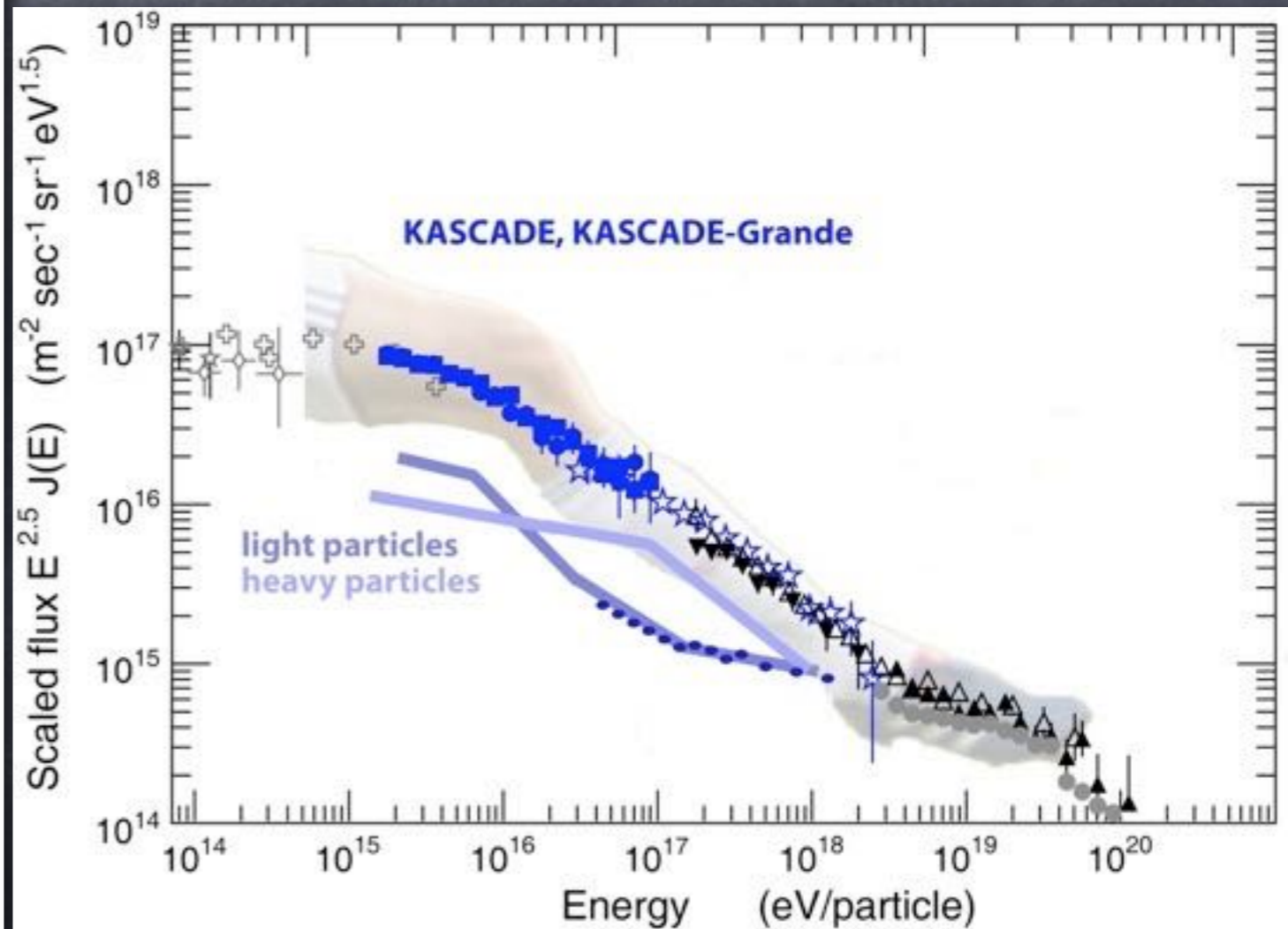
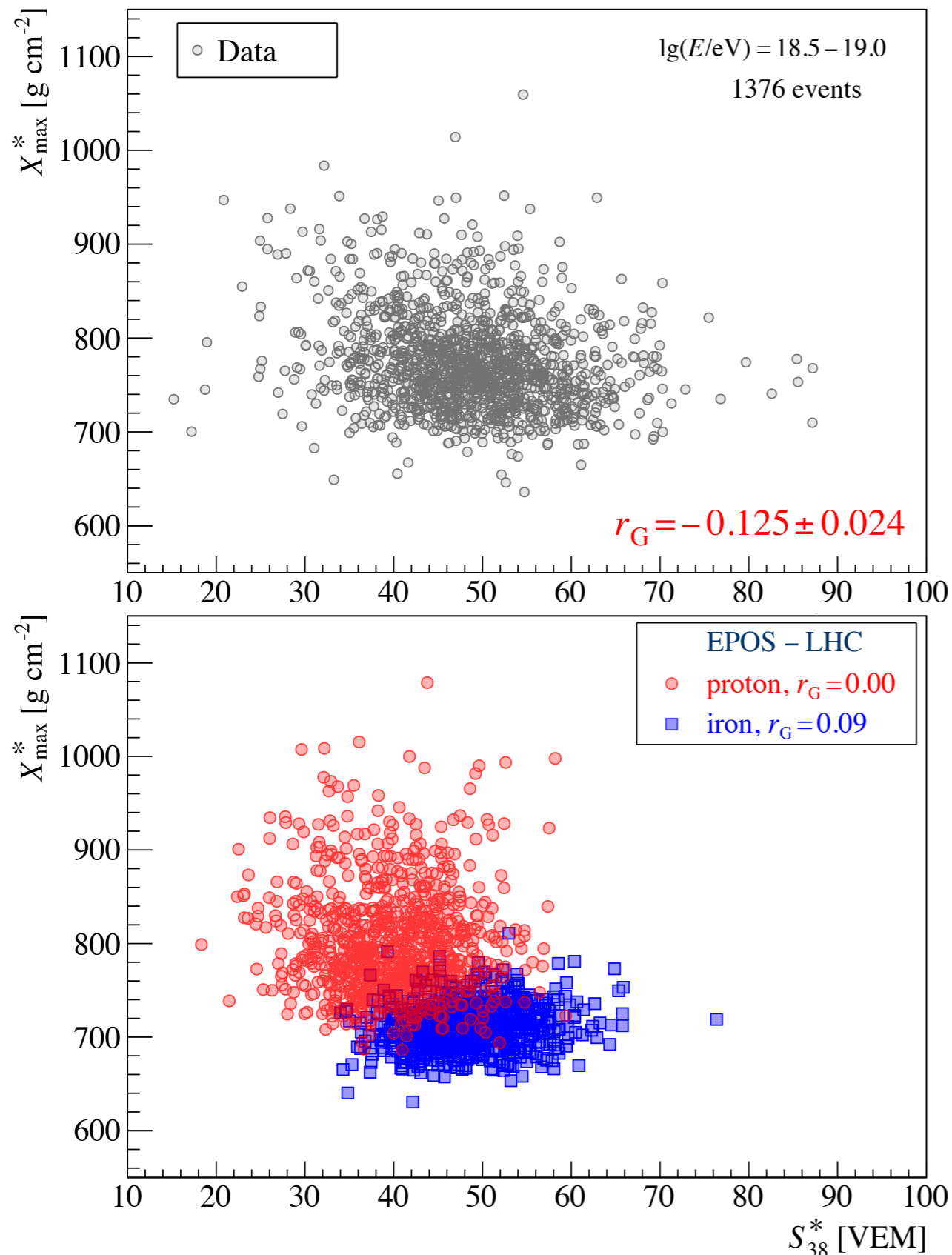


FIG. 4 (color online). The all-particle and electron-rich spectra from the analysis [8] in comparison to the results of this analysis with higher statistics. In addition to the light and heavy spectrum based on the separation between He and CNO, the light spectrum based on the separation on He is also shown. The error bars show the statistical uncertainties.

KASCADE Collaboration, Phys.Rev. D87 (2013) 081101,



Latest Pierre Auger results suggest mixed composition around the Ankle

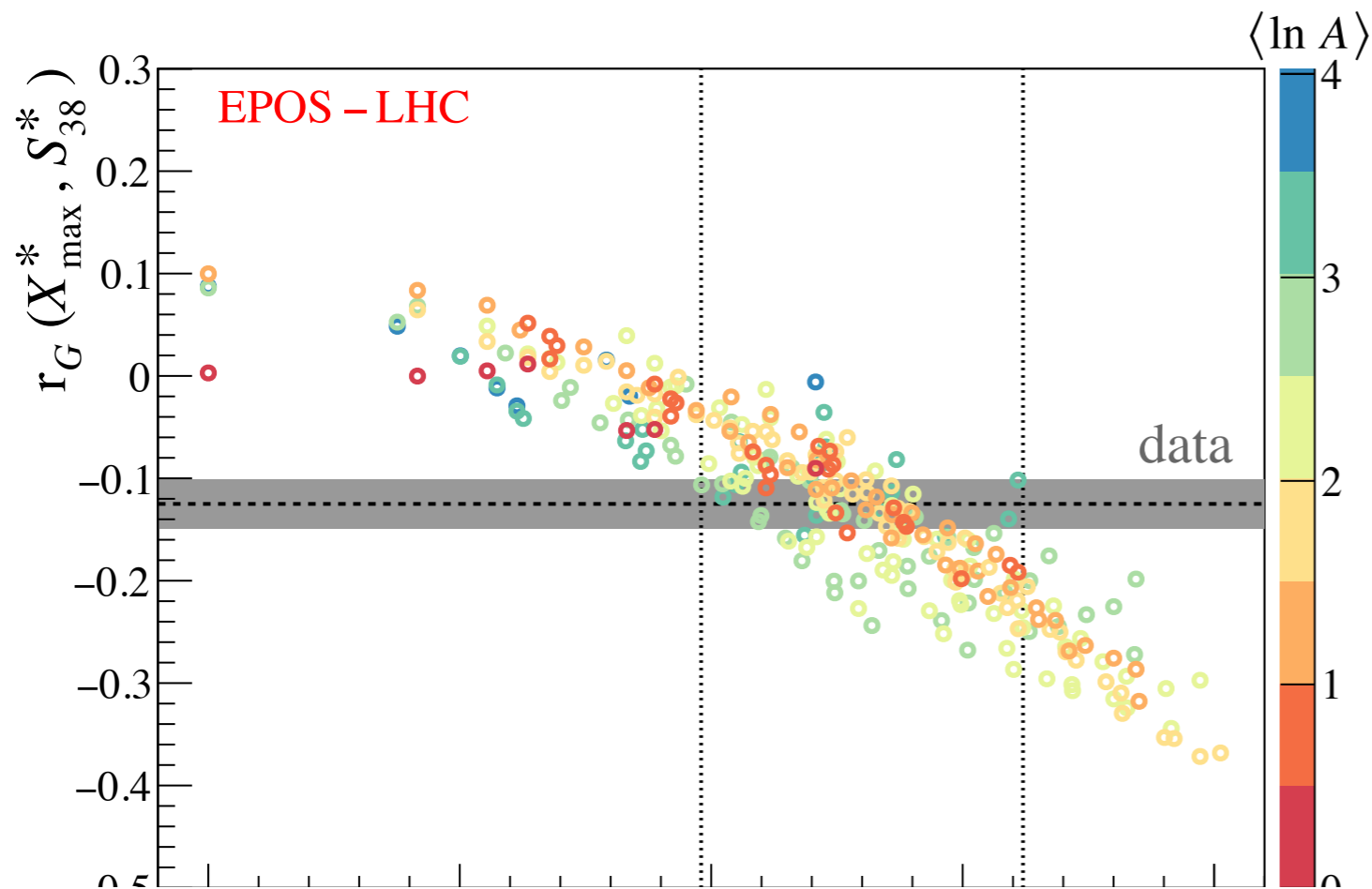


correlation between shower depth (measured by fluorescence detector) and particle density at 1km from shower core (measured by ground array) which is proxy for muon number is relatively insensitive to hadronic interaction models

Energy and zenith angle dependencies are projected out by scaling to 10 EeV and zenith angle 38 degrees.

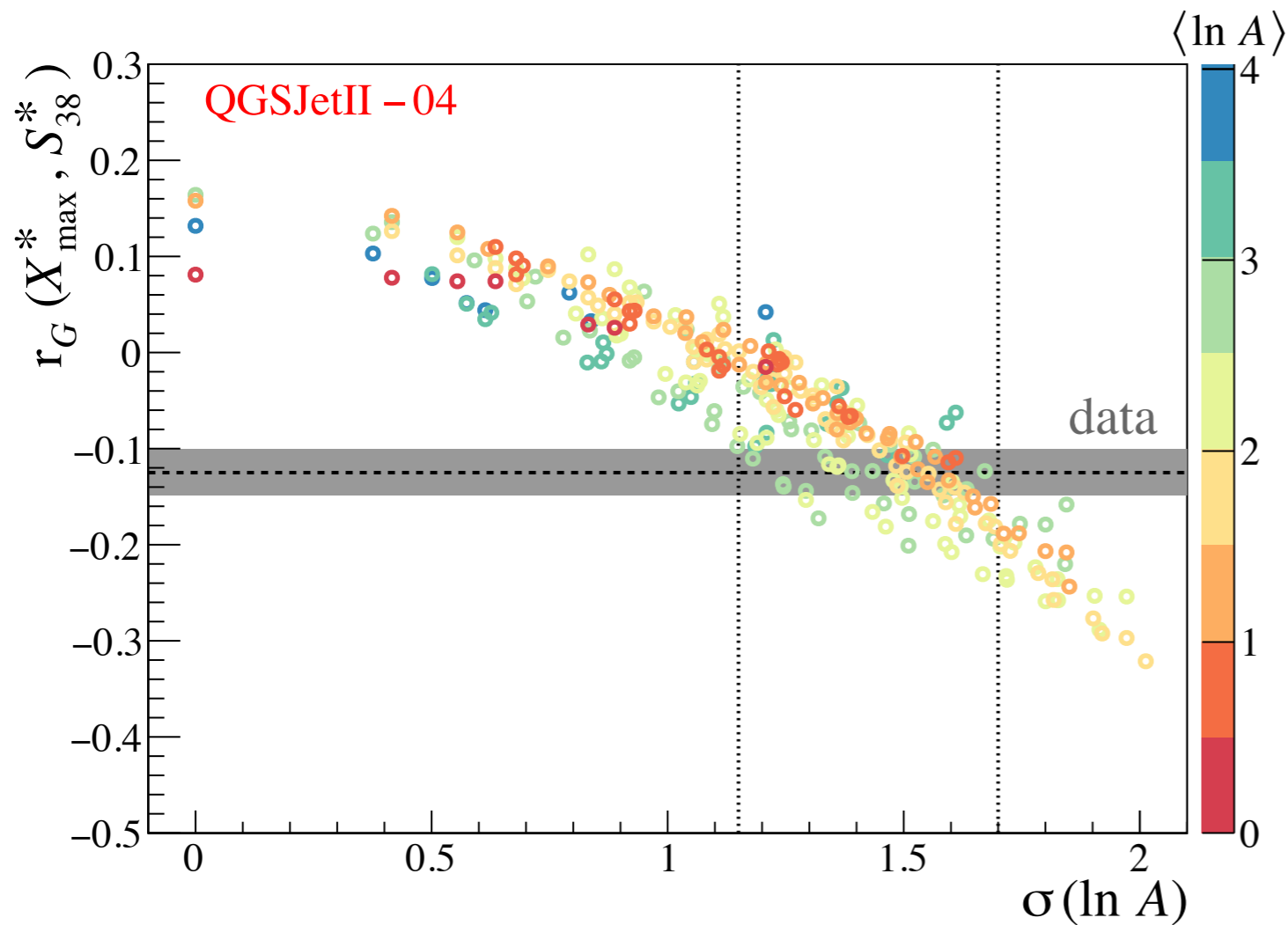
Pure composition: zero or positive correlation
mixed composition: negative correlation because large X_{\max} correlates with light nuclei and small muon abundance

Pierre Auger collaboration, Phys. Lett. B 762, 288 (2016) [arXiv:1609.08567]

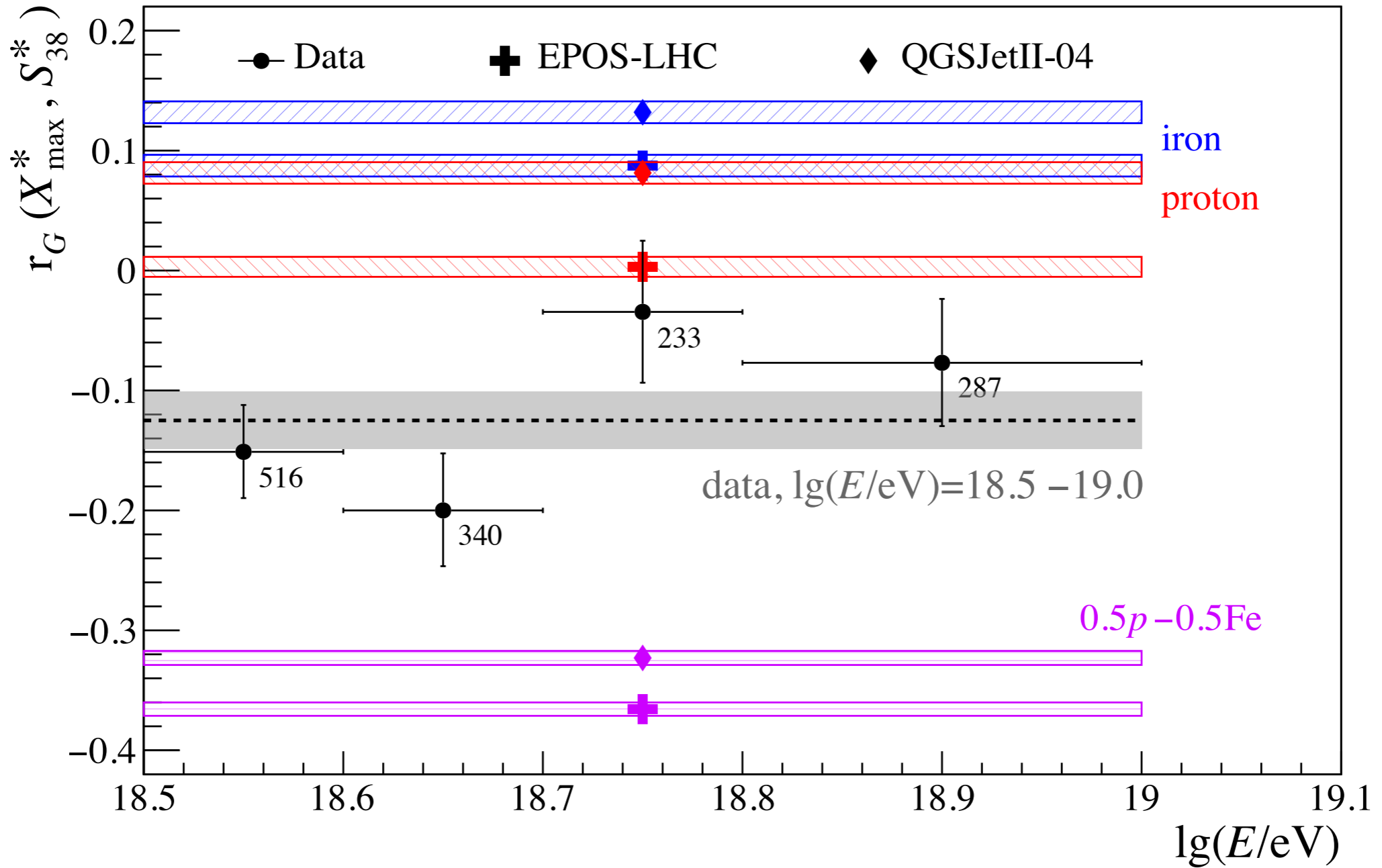


correlation coefficient versus measure of width of mass distribution: larger spread of masses leads to smaller correlation coefficients

The observed correlations indicate a mixed composition including nuclei heavier than helium, $A > 4$ with mass spread $\sigma(\ln A) = 1.35 \pm 0.35$



Summary of correlation coefficient: no significant energy trend



recent compilation of individual element spectra

S. Thoudam et al., arXiv:1605.03111

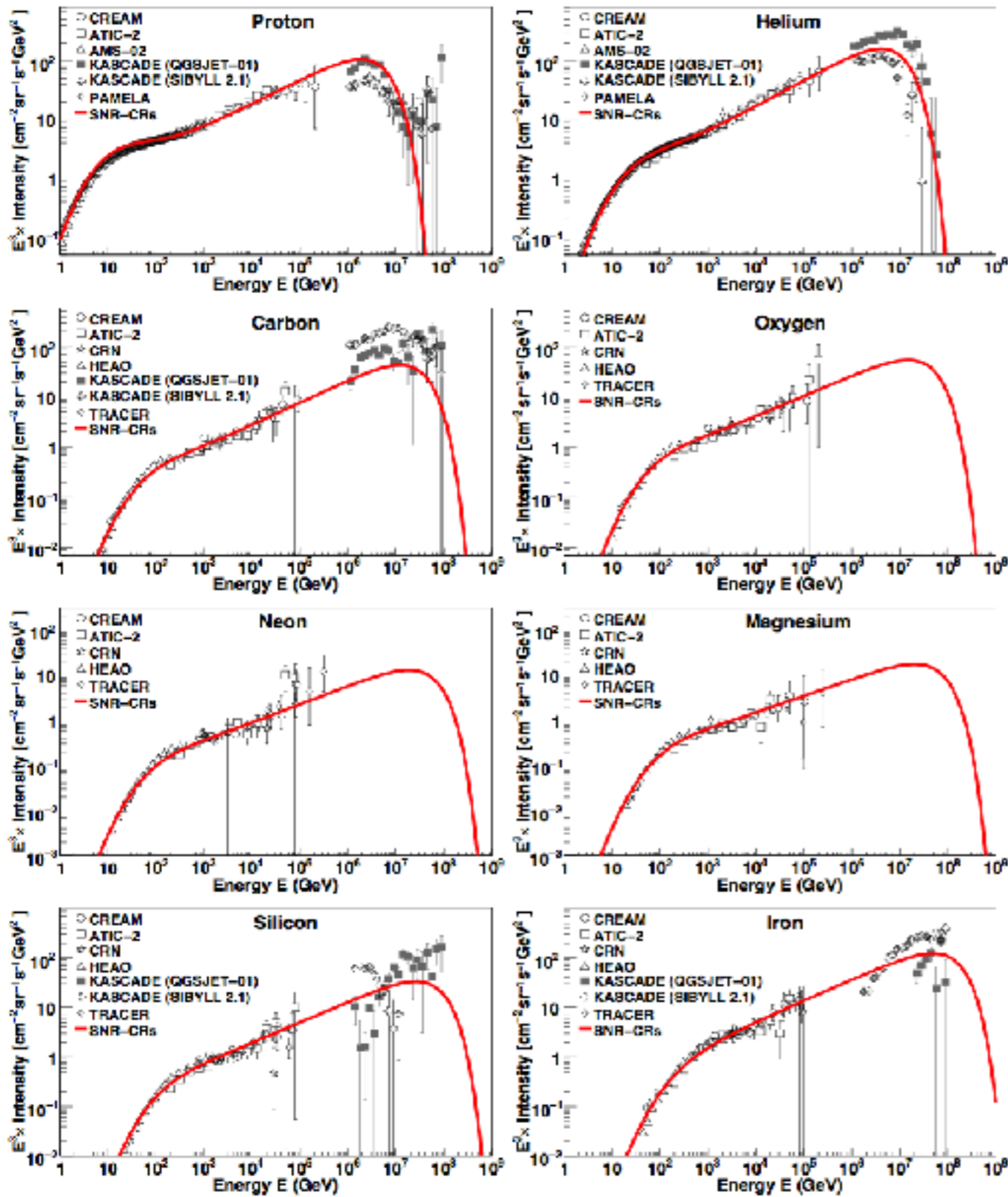


Fig. 1. Energy spectra for different cosmic ray elements. Solid line: Model prediction for the SNR-CRs. Data: CREAM (Ahm et al. 2009; Yoon et al. 2011), ATIC-2 (Panov et al. 2007), AMS-02 (Aguilar et al. 2015a,b), PAMELA (Adriani et al. 2011), CRN (Müller et al. 1991; Swerdly et al. 1990), HEAO (Engelmann et al. 1990), TRACER (Oberst et al. 2011), and KASCADE (Antoni et al. 2005). Cosmic-ray source parameters (z, f) used in the calculation are given in Table 1. For the other model parameters (μ_0, a, η, s) , see text for details.

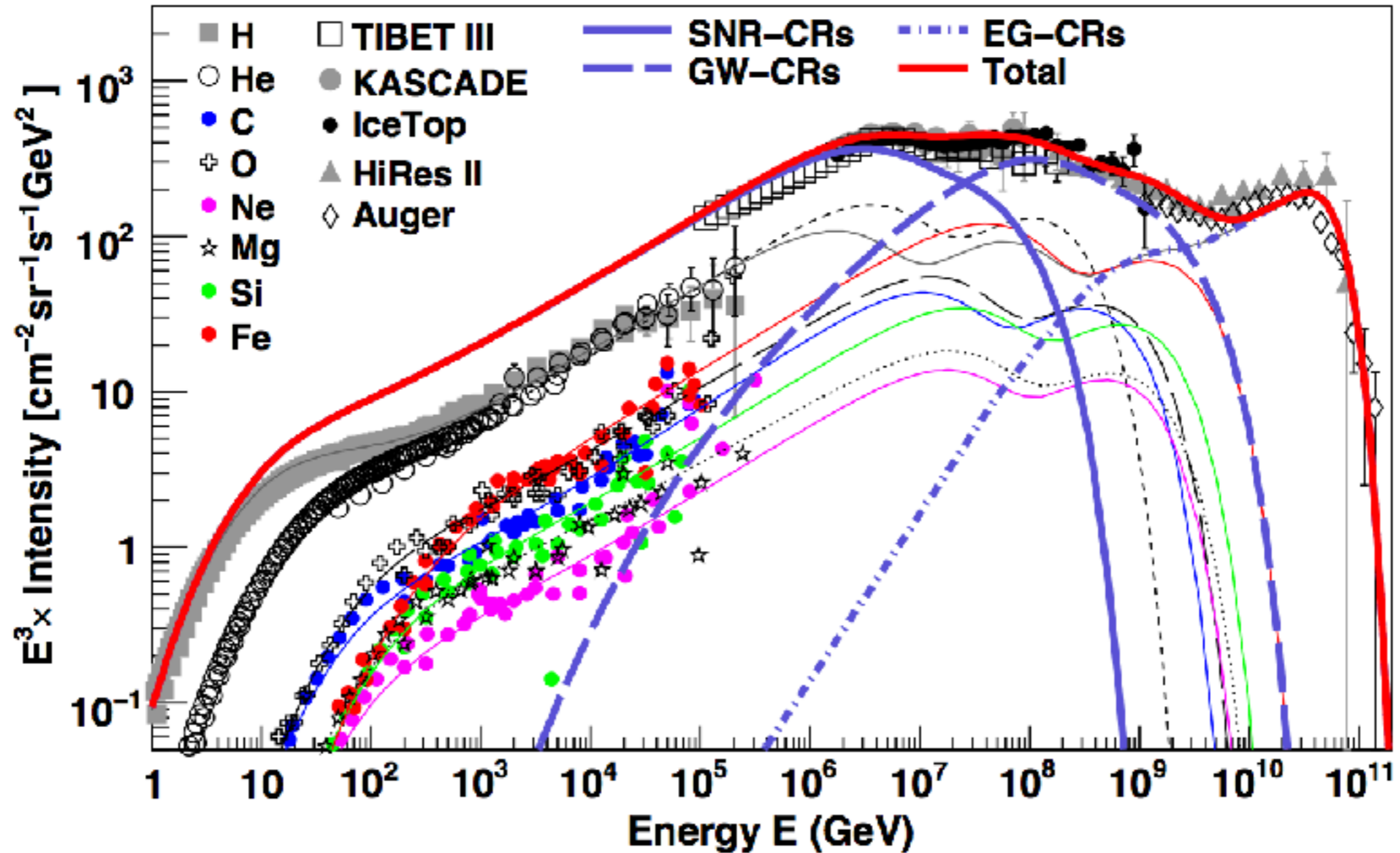


Fig. 5. Model prediction for the all-particle spectrum using the Galactic wind re-acceleration model. The thick solid blue line represents the total SNR-CRs, the thick dashed line represents GW-CRs, the thick dotted-dashed line represents EG-CRs, and the thick solid red line represents the total all-particle spectrum. The thin lines represent total spectra for the individual elements. For the SNR-CRs, an exponential energy cut-off for protons at $E_c = 3 \times 10^6$ GeV is assumed. See text for the other model parameters. Data are the same as in Figure 2.

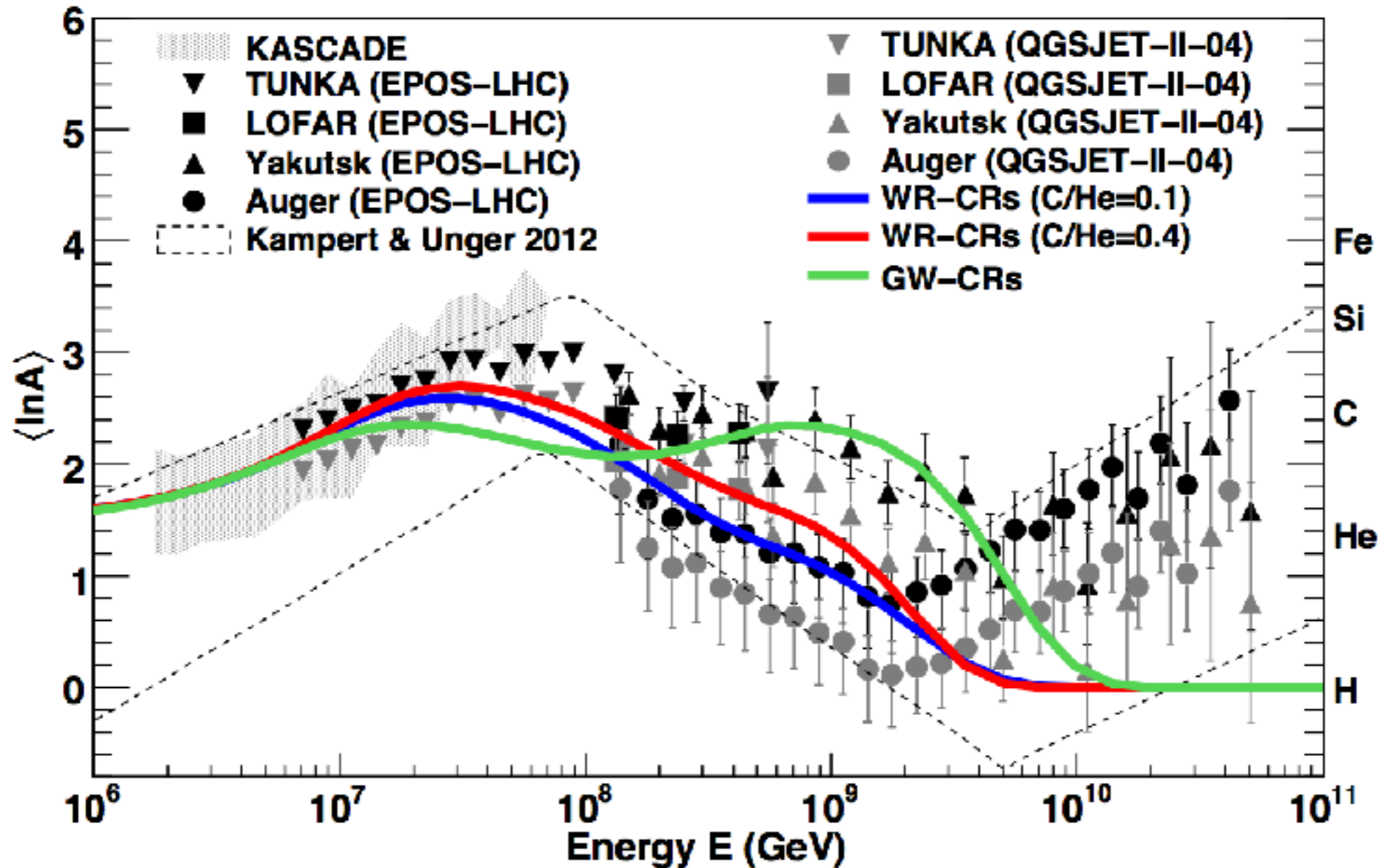


Fig. 8. Mean logarithmic mass, $\langle \ln A \rangle$, of cosmic rays predicted using the three different models of the additional Galactic component: WR-CRs ($C/He = 0.1$), WR-CRs ($C/He = 0.4$), and GW-CRs. *Data:* KASCADE (Antoni et al. 2005), TUNKA (Berezhnev et al. 2013), LOFAR (Buitink et al. 2016), Yakutsk (Knurenko & Sabourov 2010), the Pierre Auger Observatory (Porcelli et al. 2015), and the different optical measurements compiled in Kampert & Unger (2012). The two sets of data points correspond to two different hadronic interaction models (EPOS-LHC and QGSJET-II-04) used to convert X_{max} values to $\langle \ln A \rangle$.

Global Picture on Mass Composition

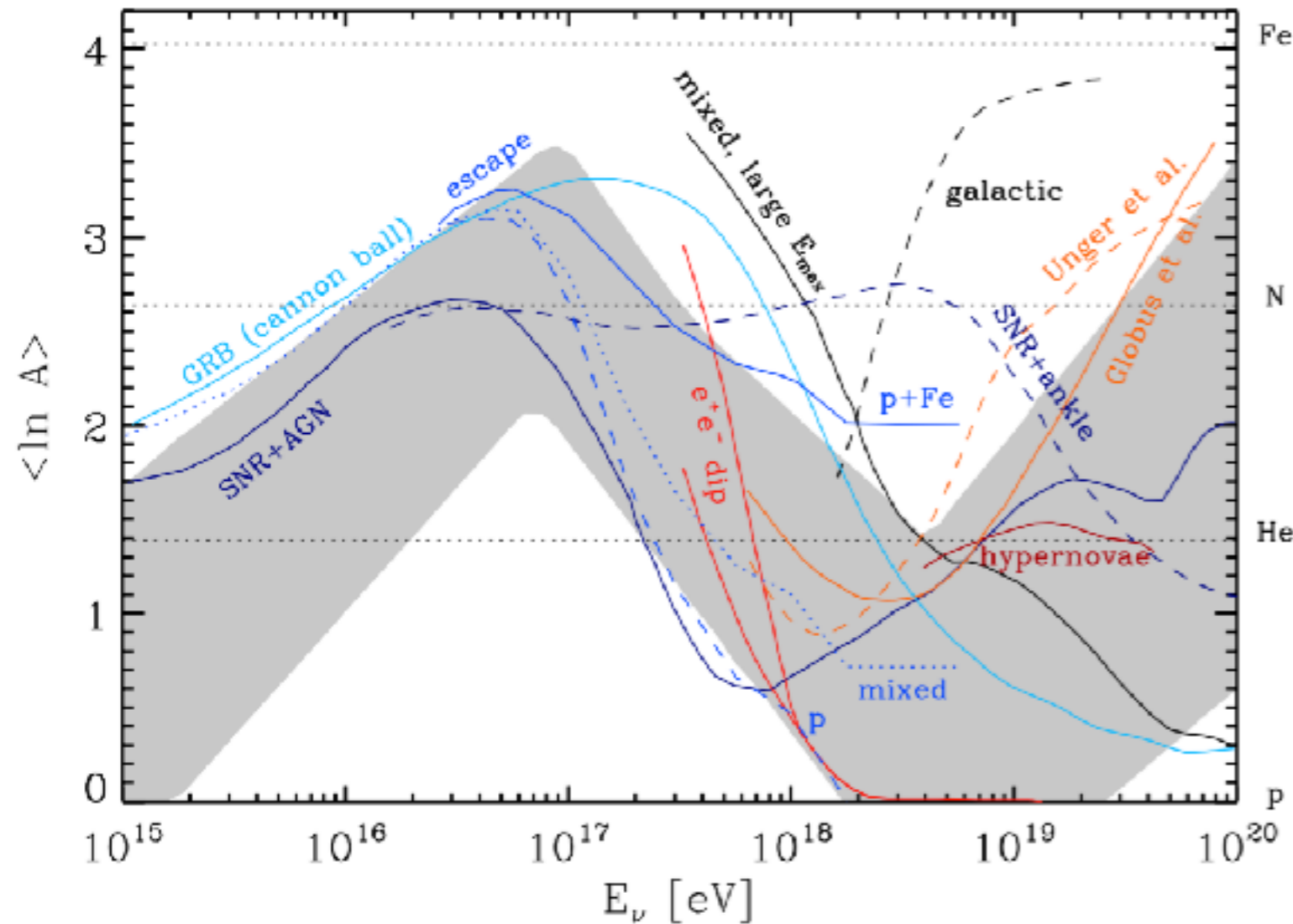


Fig. 5.8 The energy dependence of the average logarithmic mass predicted by various models, as indicated and explained in more details in the text. The grey band represents the combined uncertainties resulting from systematic experimental errors and hadronic model uncertainties, based on data such as the ones shown in Fig. 5.7. The first minimum in $\langle \ln A \rangle$ at $\simeq 3 \times 10^{15}$ eV corresponds to the CR knee and the first maximum in $\langle \ln A \rangle$ at $\simeq 10^{17}$ eV corresponds to the *second knee*. Both the knee and the second knee could signify a rigidity dependent Peters cycle either due to the maximal rigidity reached at acceleration in supernova remnants or due to a transition to a propagation regime leading to faster CR leakage from the Galaxy. Finally, the second minimum in $\langle \ln A \rangle$ at $\simeq 5 \times 10^{18}$ eV signifies the *ankle*. Compare the CR spectrum shown in Fig. 5.6. Inspired by Ref. [231].

Indications of "Peters cycles" for galactic and extragalactic sources whose maximal energies are proportional to the charge Z and extend up to $\sim 10^{17}$ and 10^{20} eV, respectively

G. Sigl, book to appear

see also K.-H.Kampert and M.Unger, *Astropart.Phys.* 35 (2012) 660

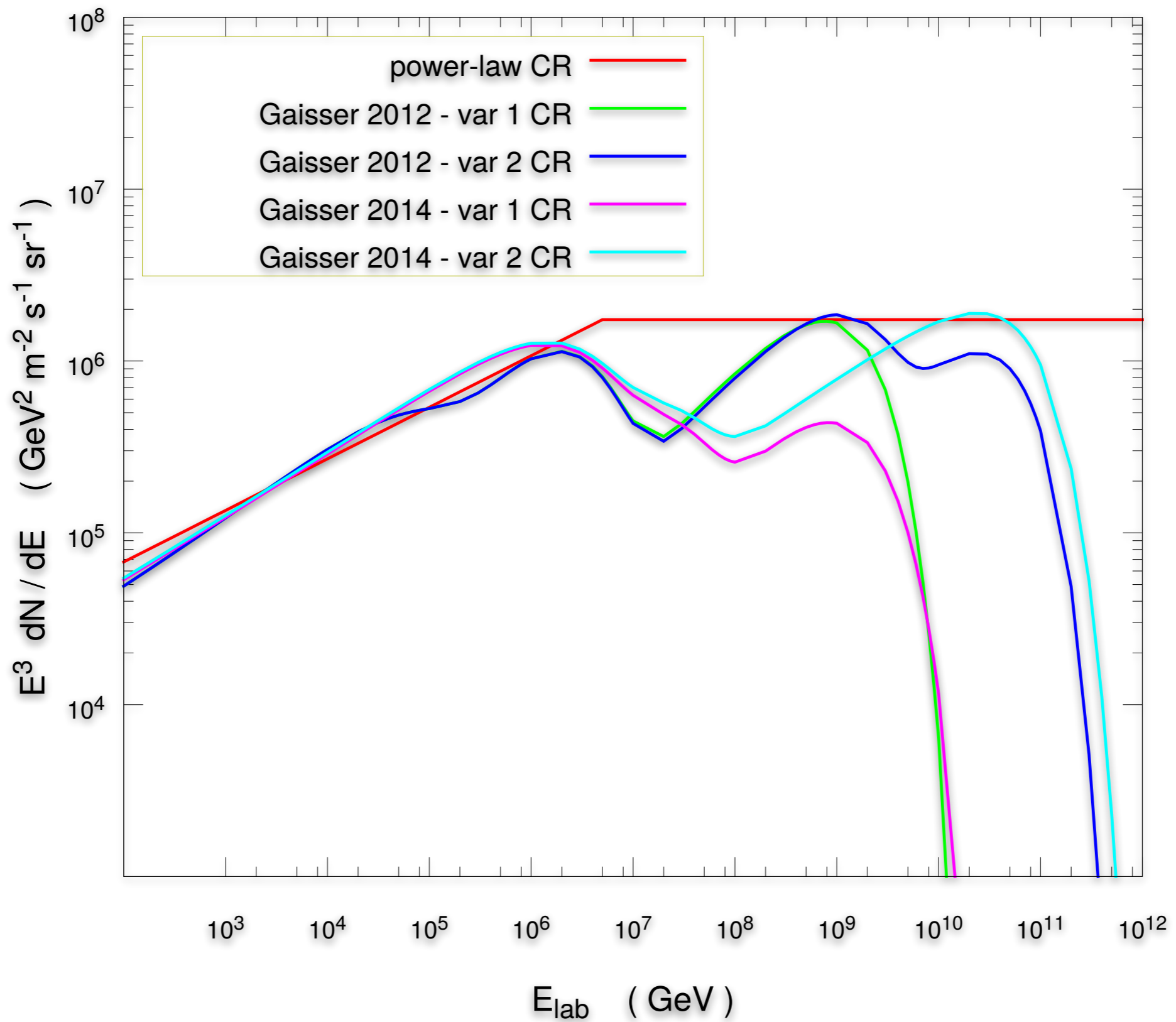
Light Galactic Nuclei produce too much anisotropy above $\approx 10^{18}$ eV. This implies:

1.) if composition around 10^{18} eV is light \Rightarrow probably extragalactic and ankle may be due to pair production by protons, but this scenario is now strongly disfavoured by Pierre Auger finding mixed composition at the ankle

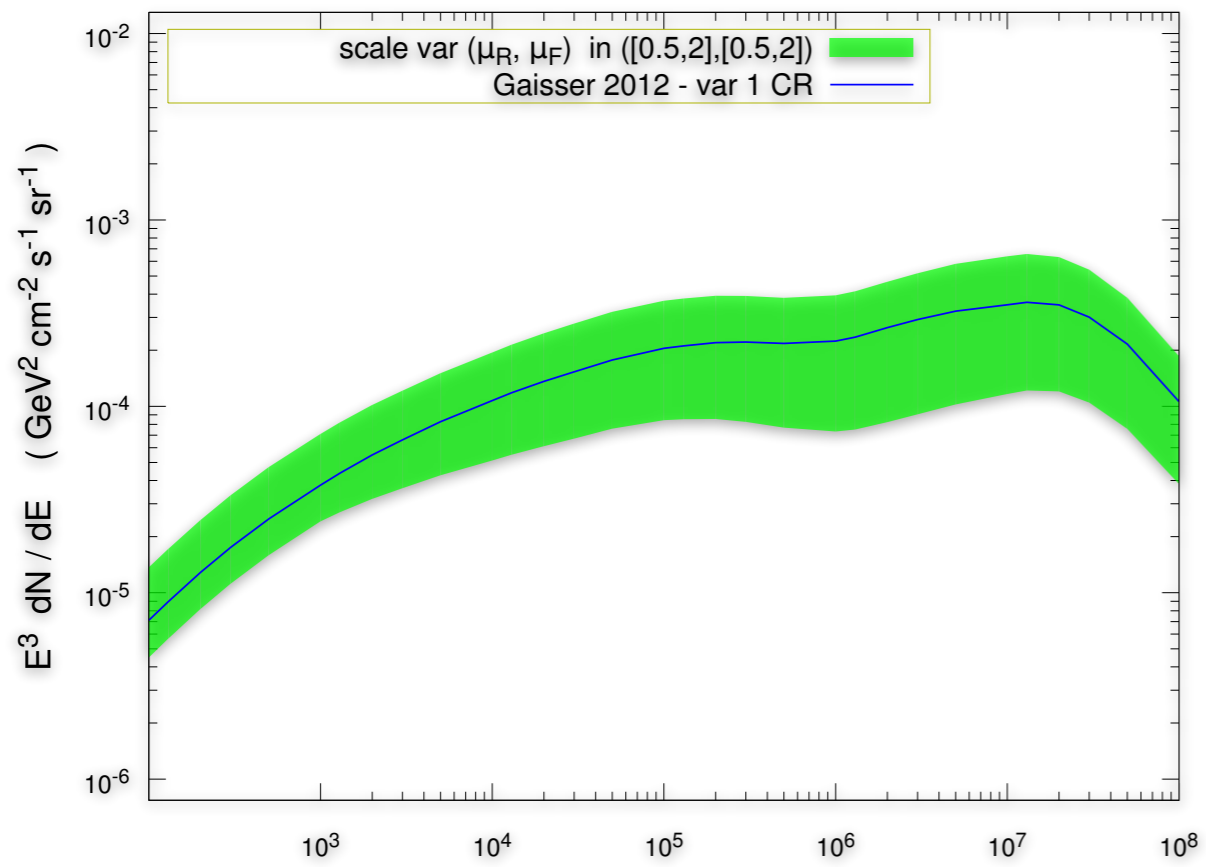
2.) if composition around 10^{18} eV is heavy \Rightarrow transition could be at the ankle if Galactic nuclei are produced by sufficiently frequent transients, e.g. magnetars

Flux models used in this work

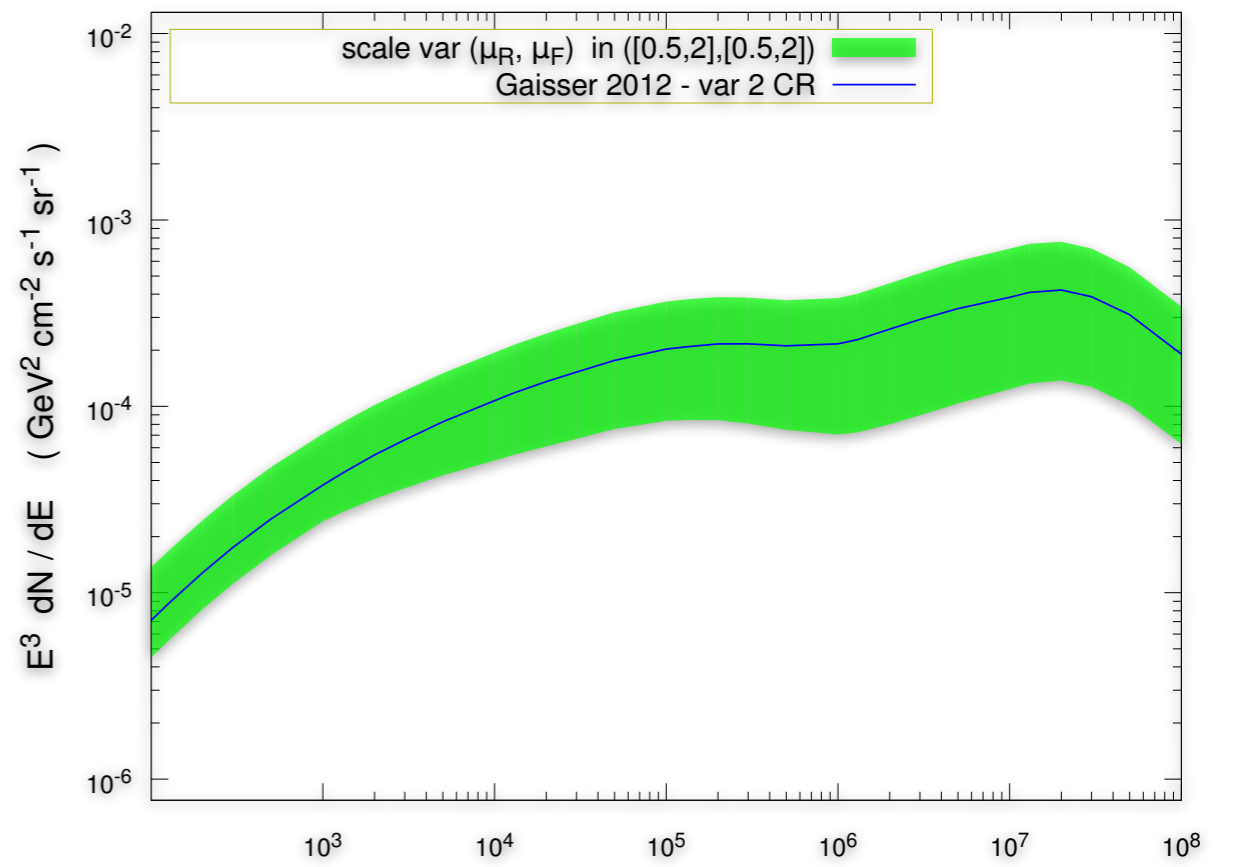
Cosmic Ray primary all-nucleon flux



$\nu_\mu + \text{anti-}\nu_\mu$ flux



$\nu_\mu + \text{anti-}\nu_\mu$ flux



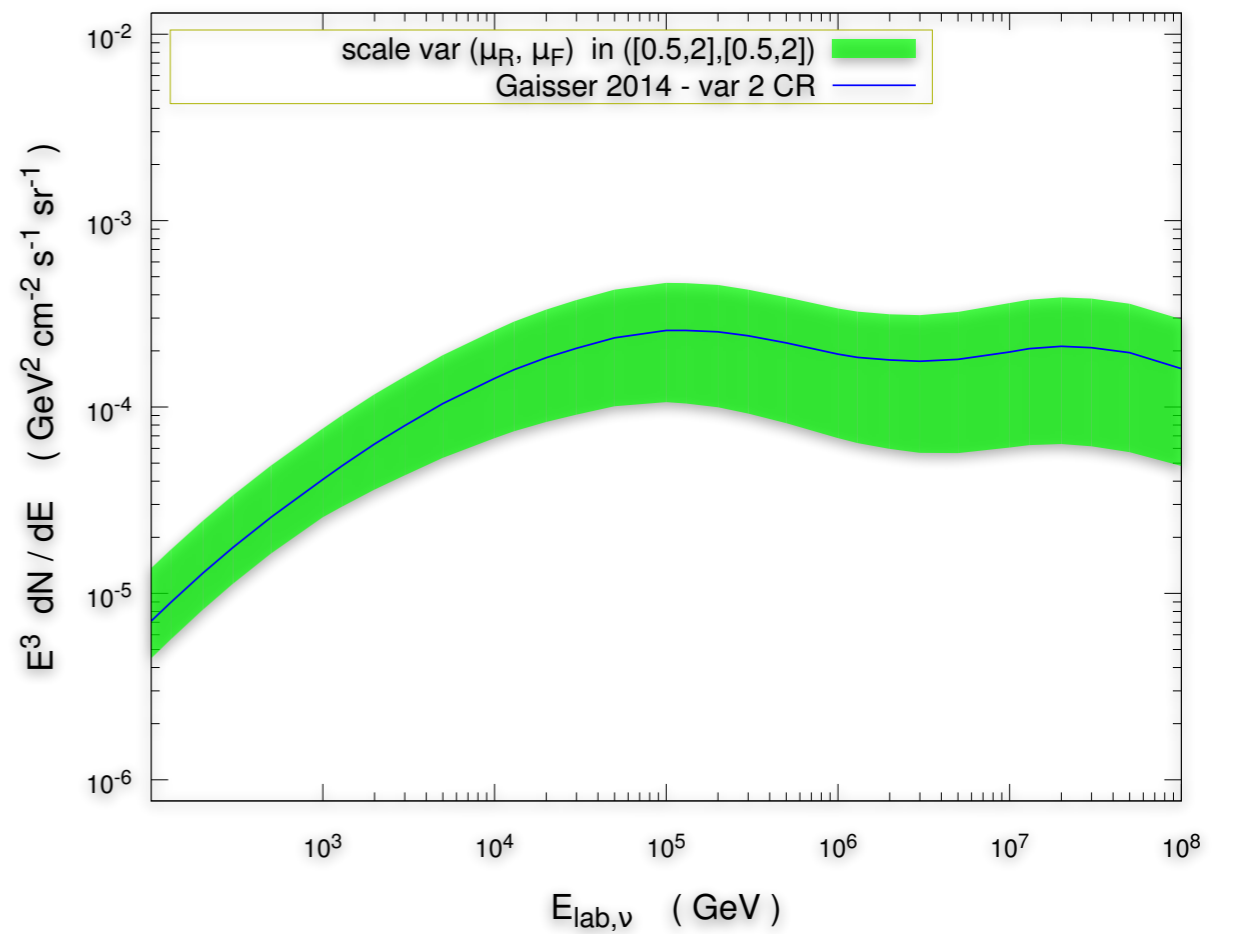
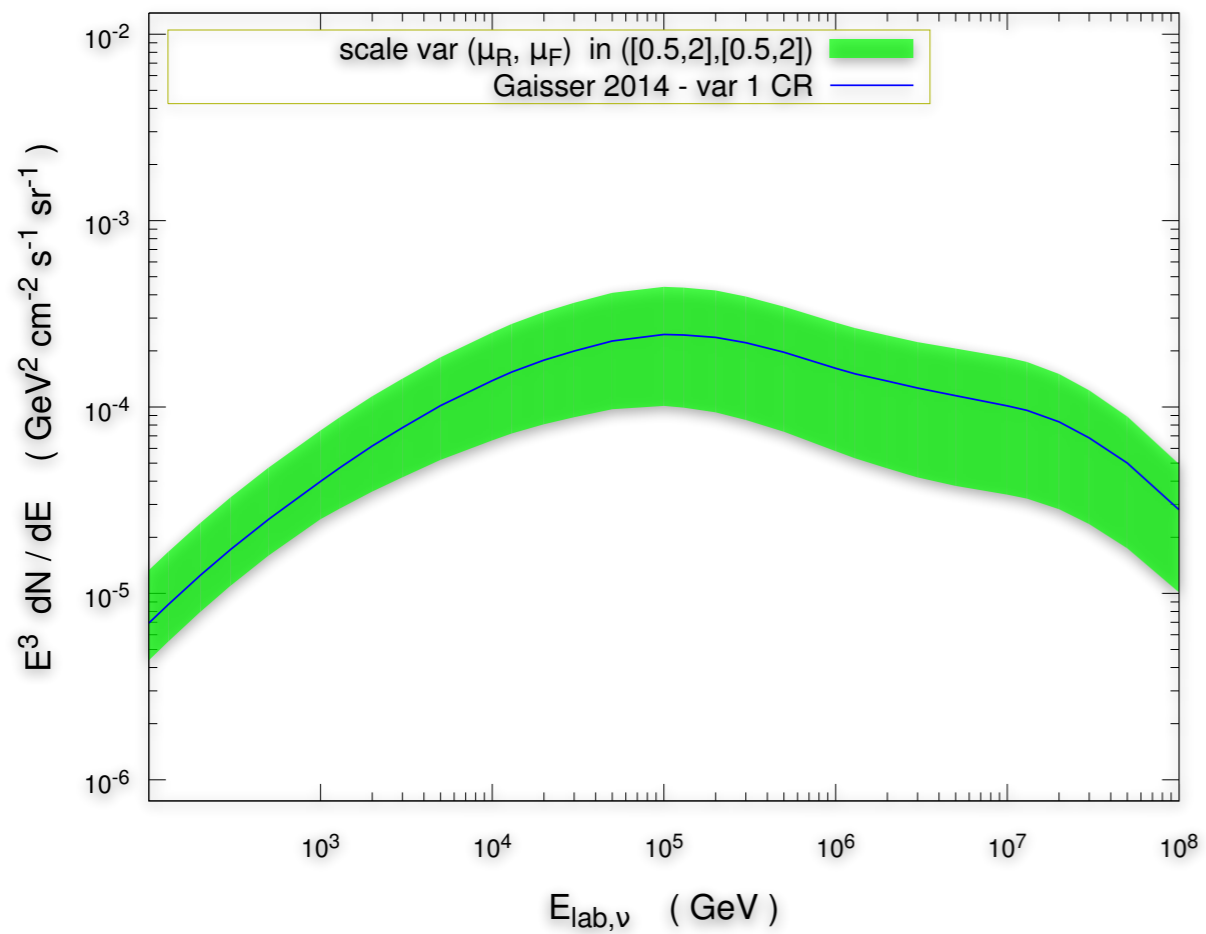
$E_{\text{lab},\nu}$ (GeV)

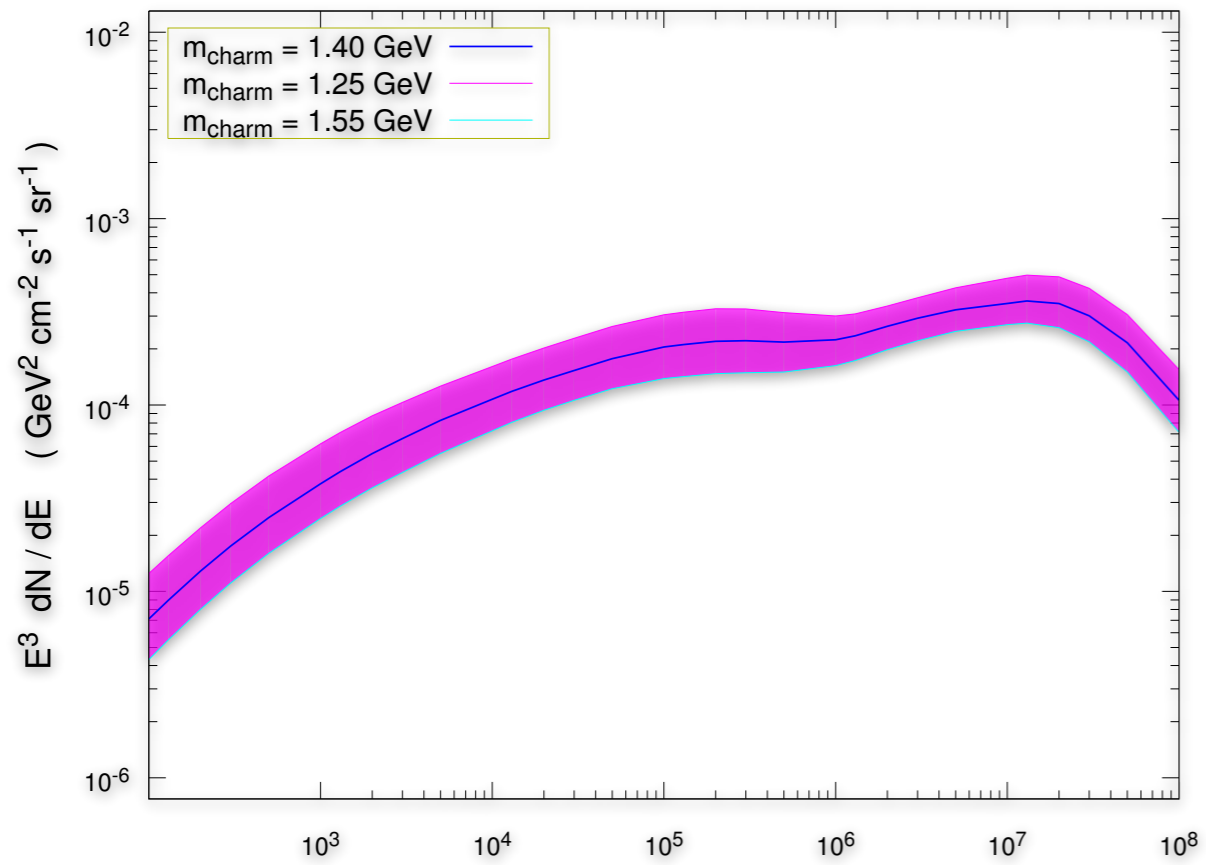
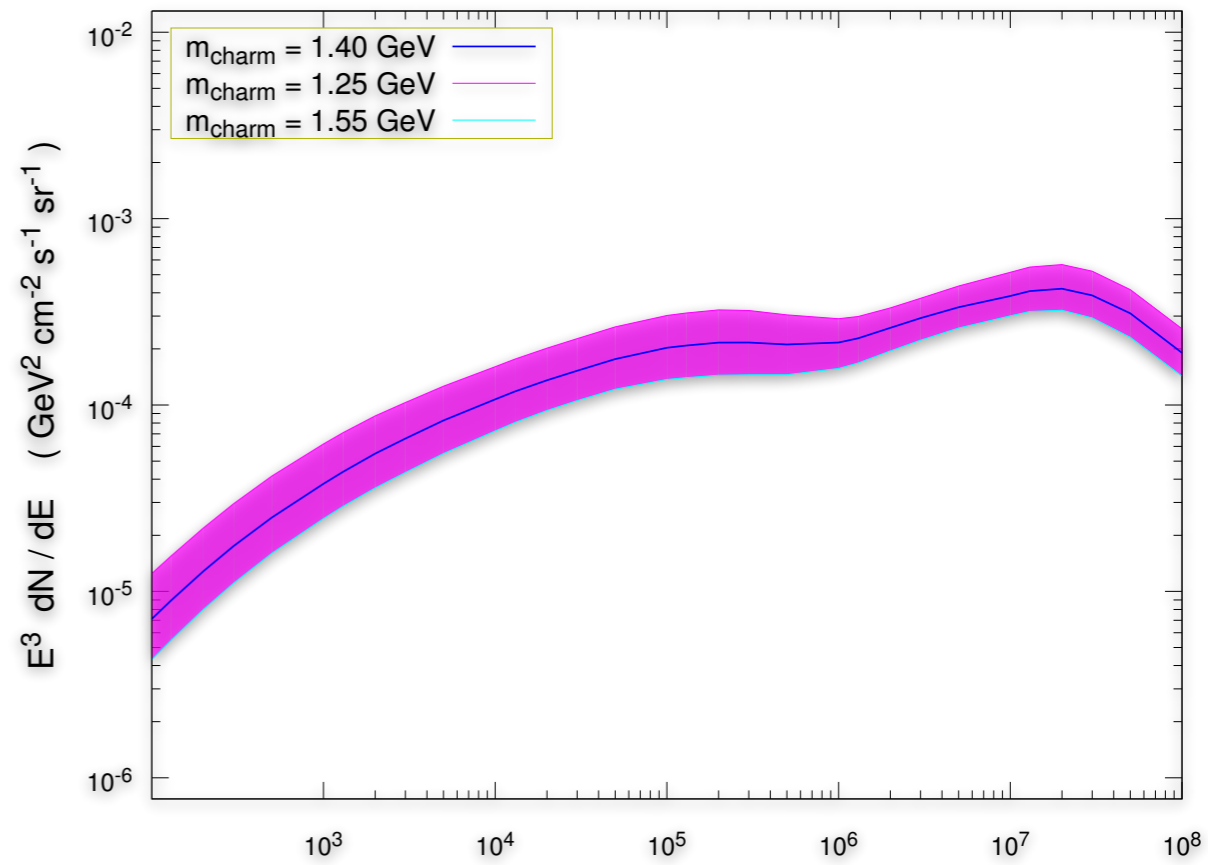
$\nu_\mu + \text{anti-}\nu_\mu$ flux

renormalization and factorisation scale variation

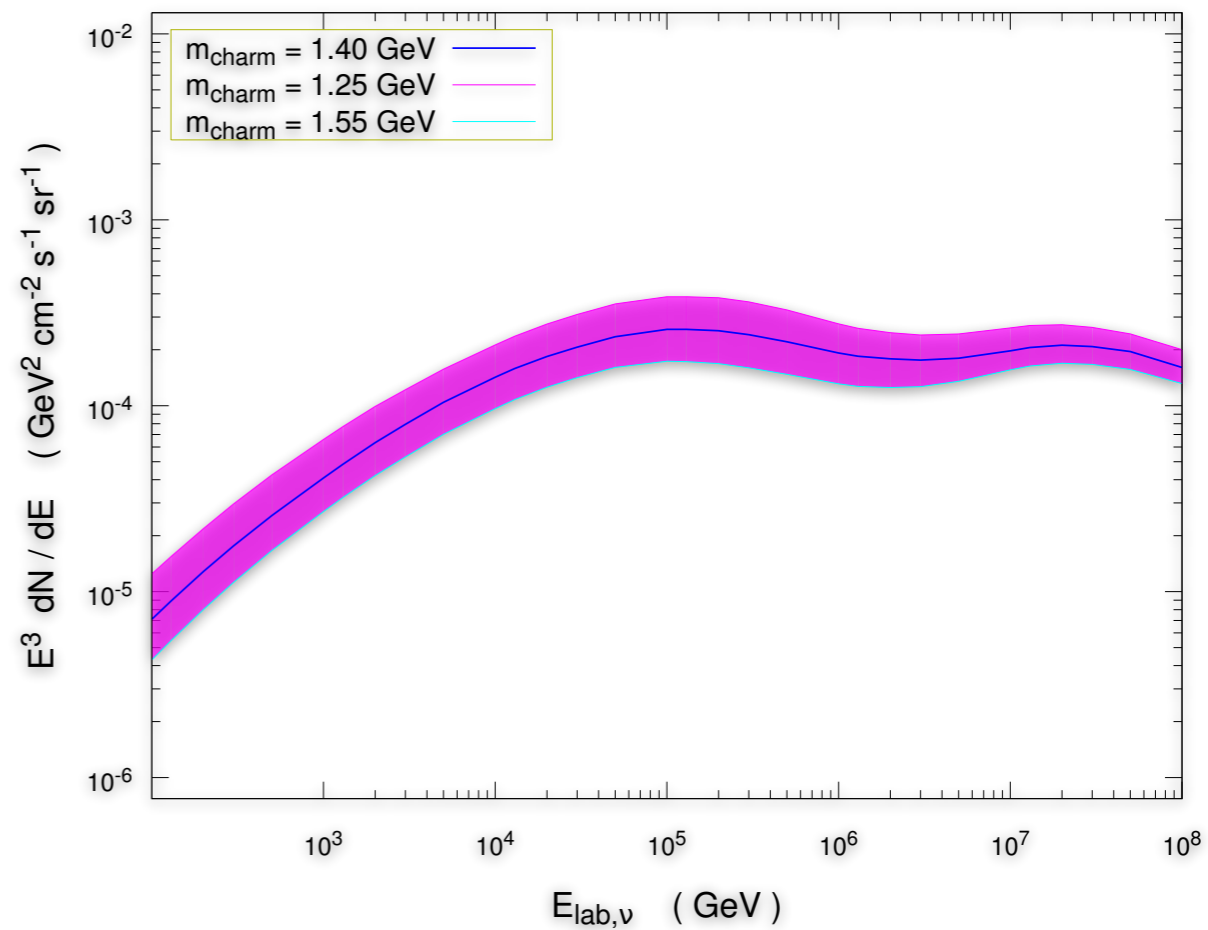
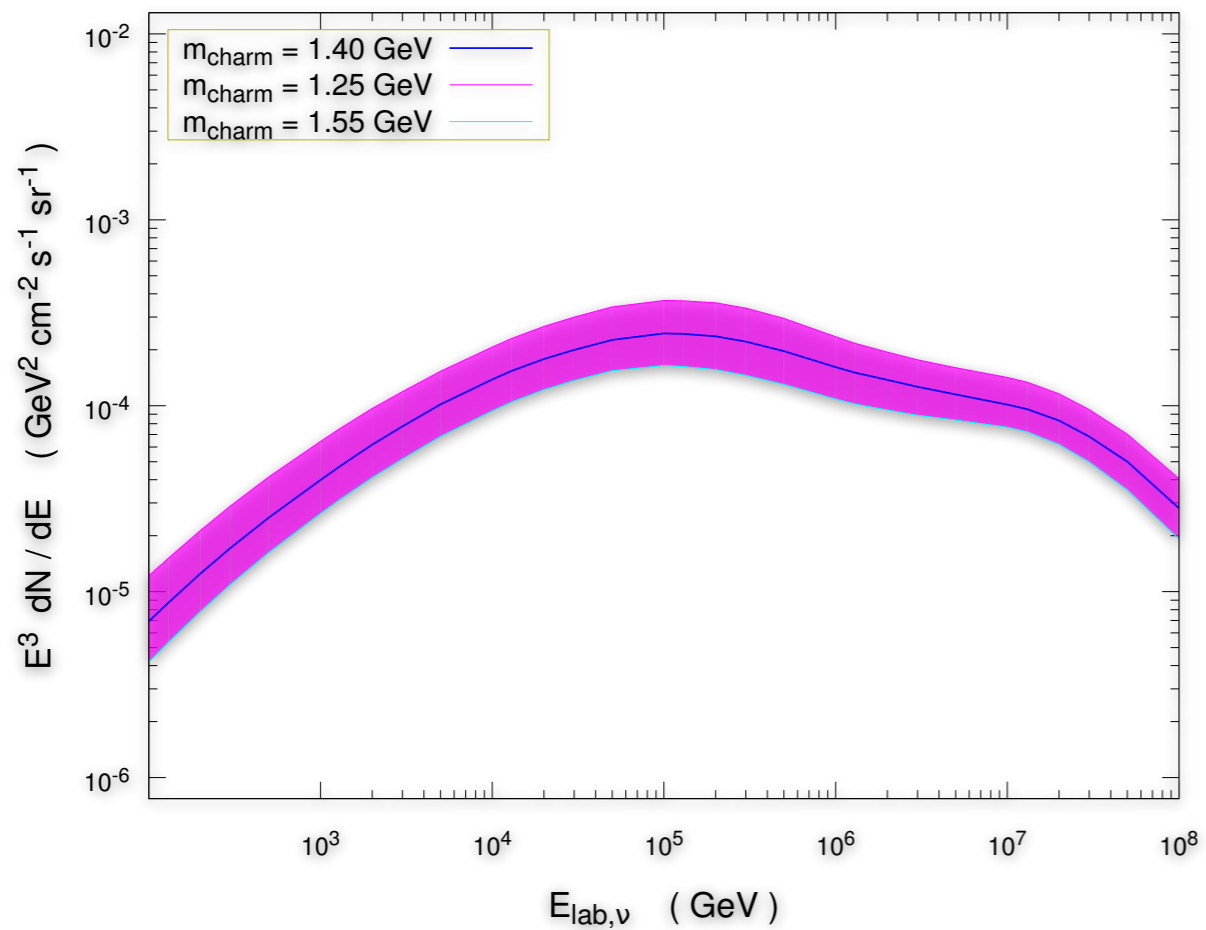
$E_{\text{lab},\nu}$ (GeV)

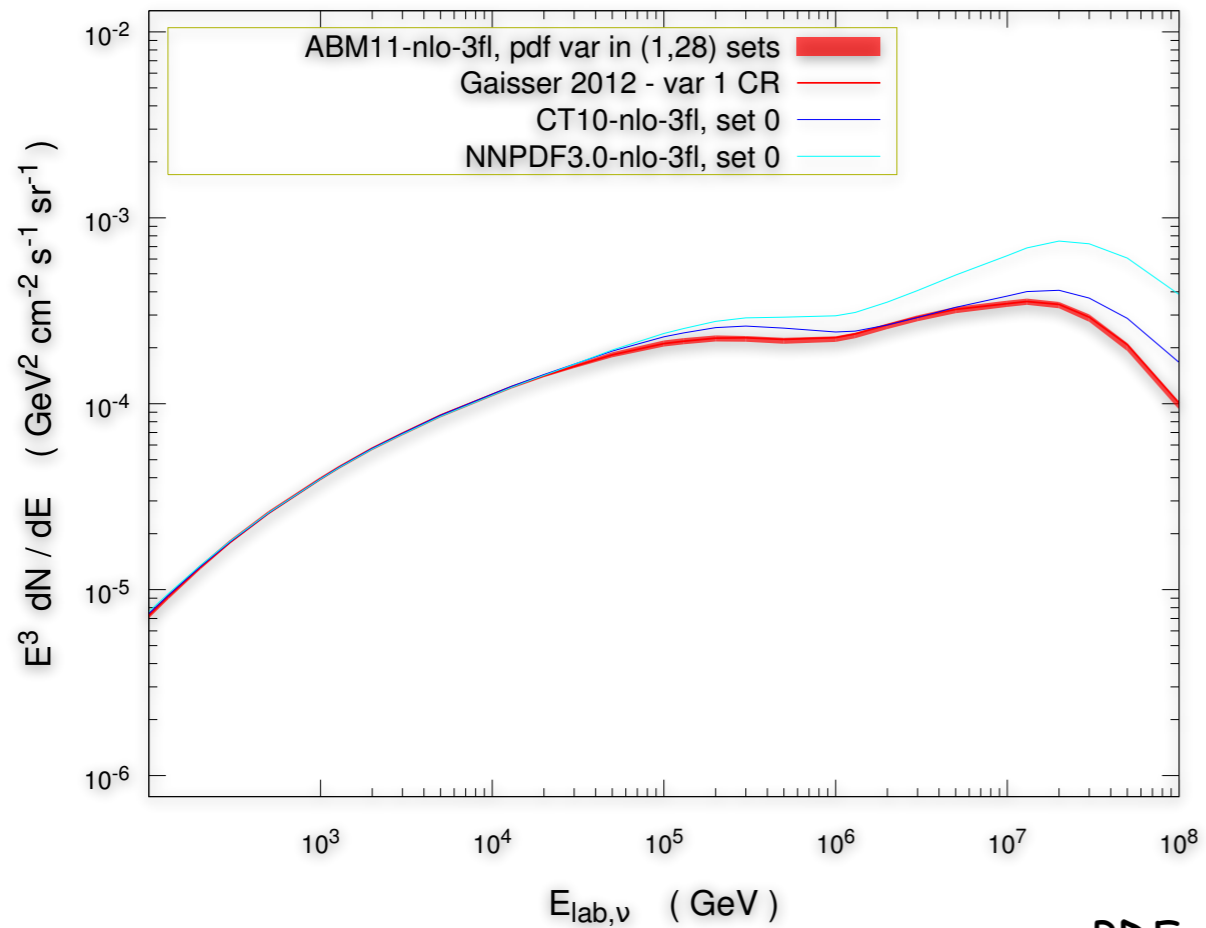
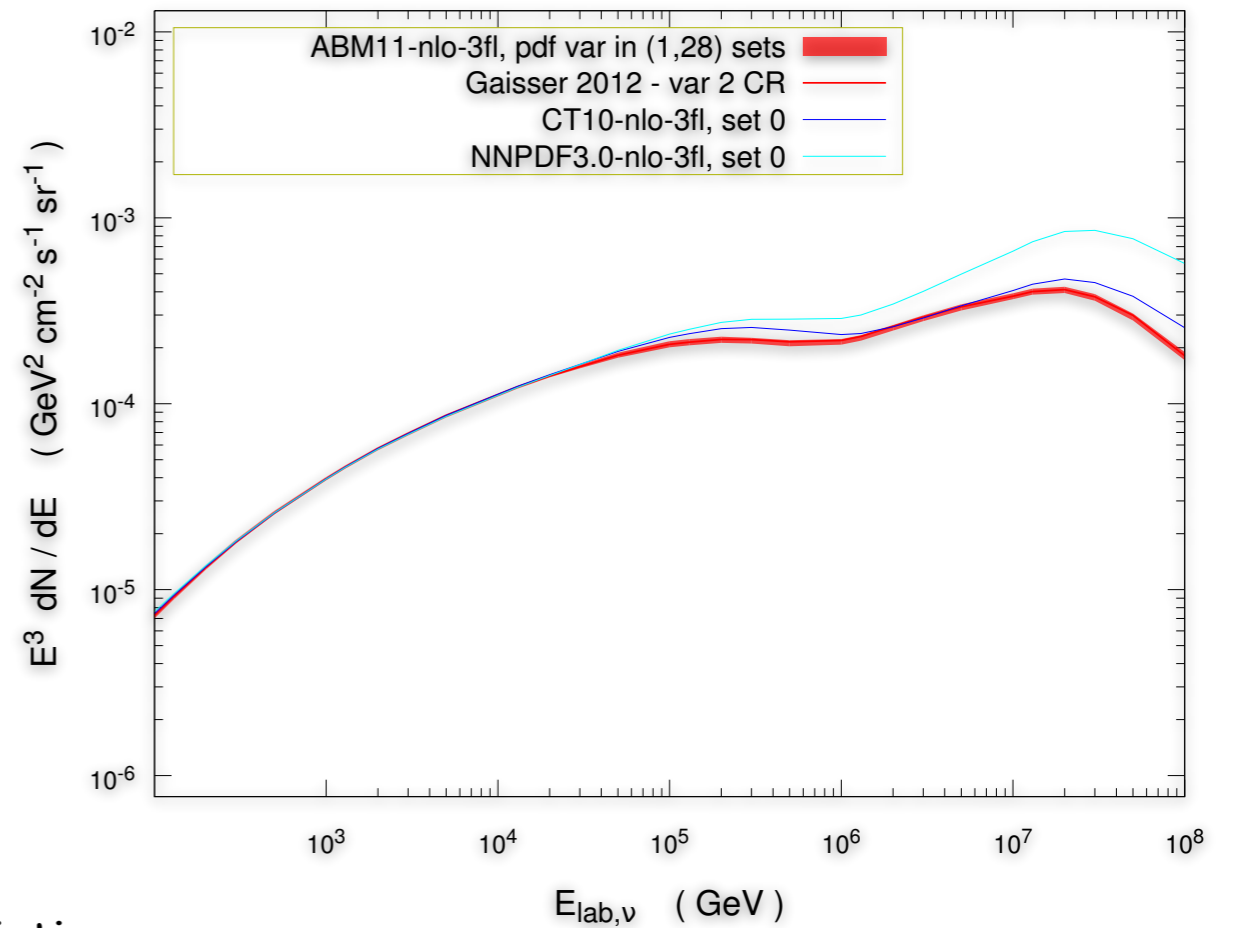
$\nu_\mu + \text{anti-}\nu_\mu$ flux



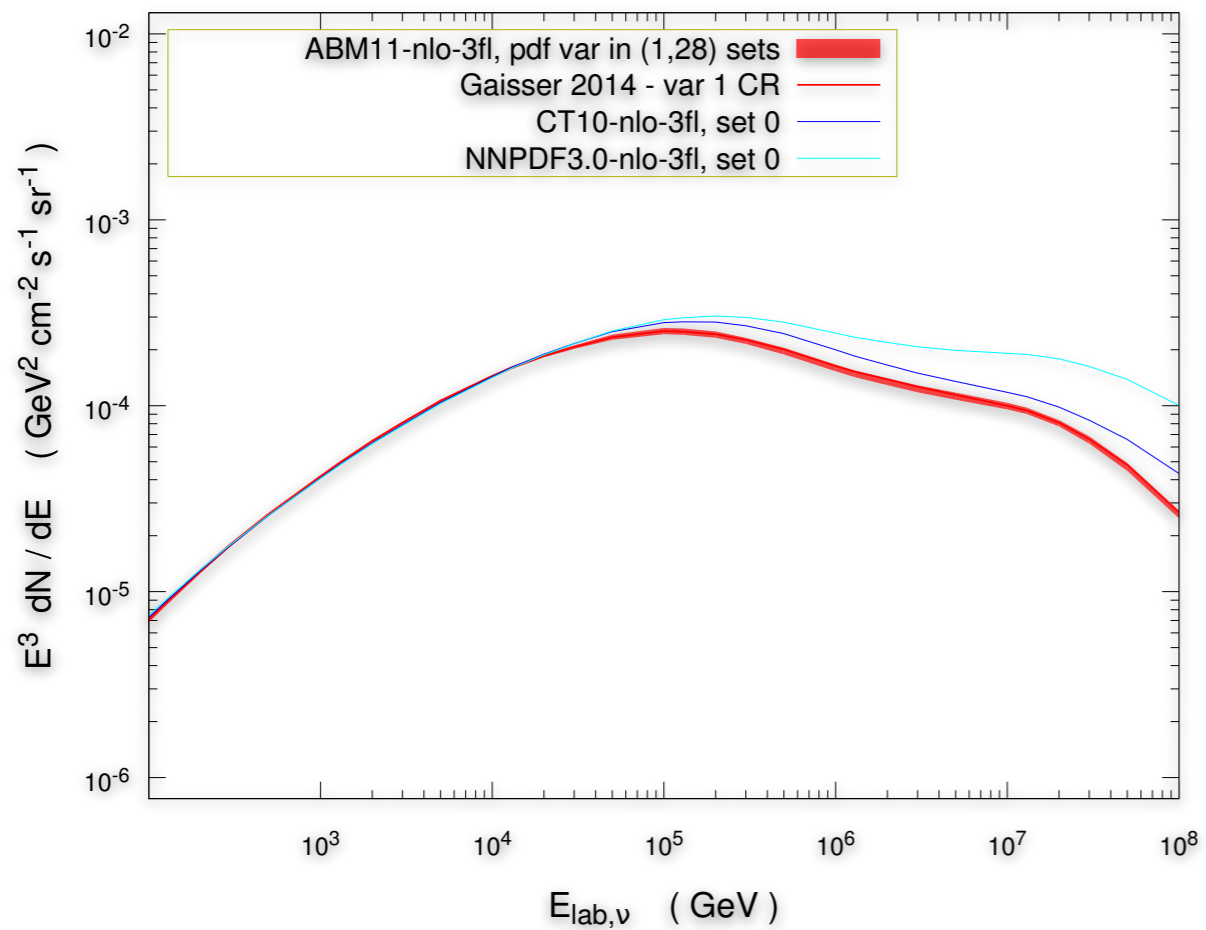
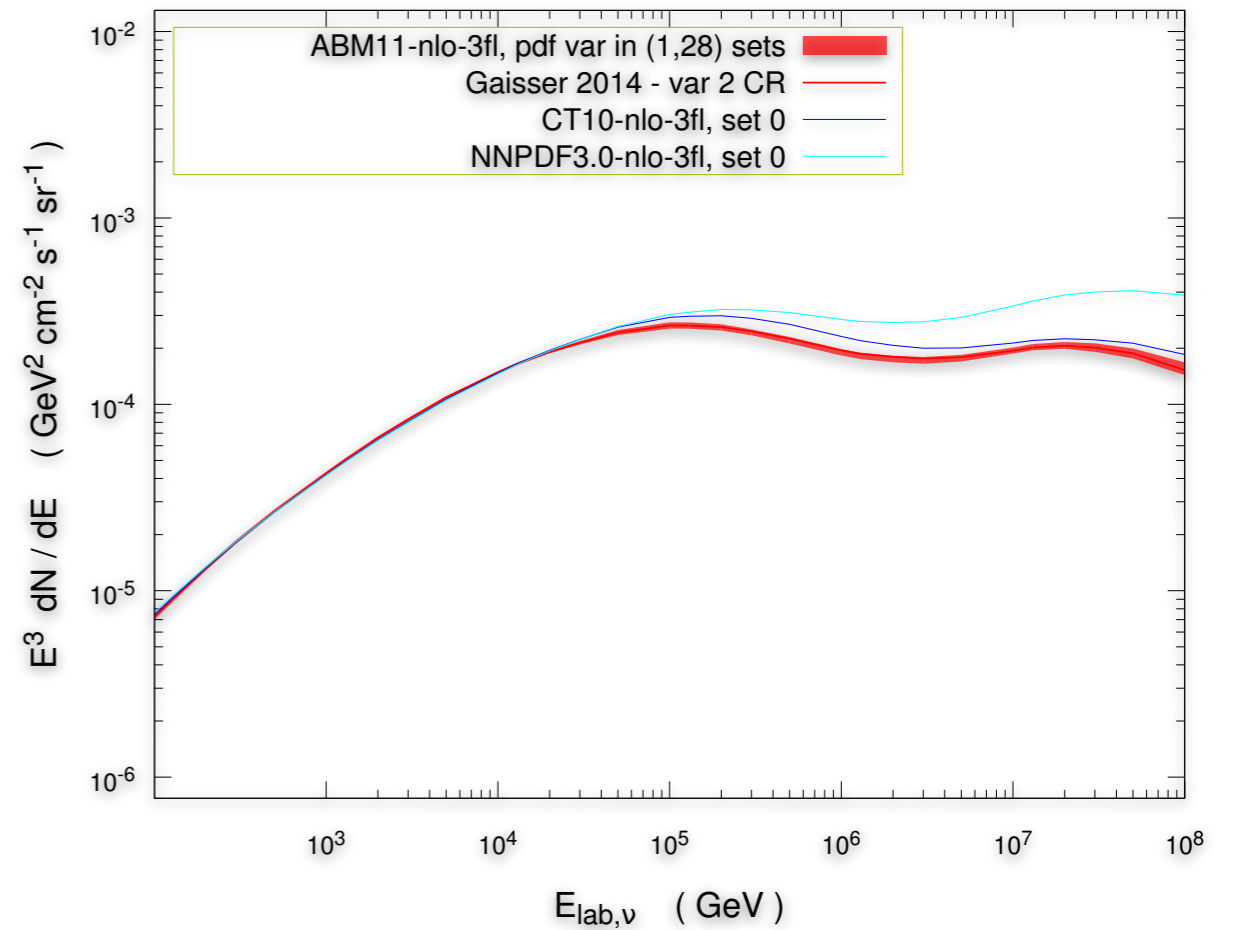
$\nu_\mu + \text{anti-}\nu_\mu$ flux $\nu_\mu + \text{anti-}\nu_\mu$ flux $E_{\text{lab},\nu}$ (GeV)
 $\nu_\mu + \text{anti-}\nu_\mu$ flux

charm quark pole mass variation

 $E_{\text{lab},\nu}$ (GeV)
 $\nu_\mu + \text{anti-}\nu_\mu$ flux

$\nu_\mu + \text{anti-}\nu_\mu$ flux $\nu_\mu + \text{anti-}\nu_\mu$ flux

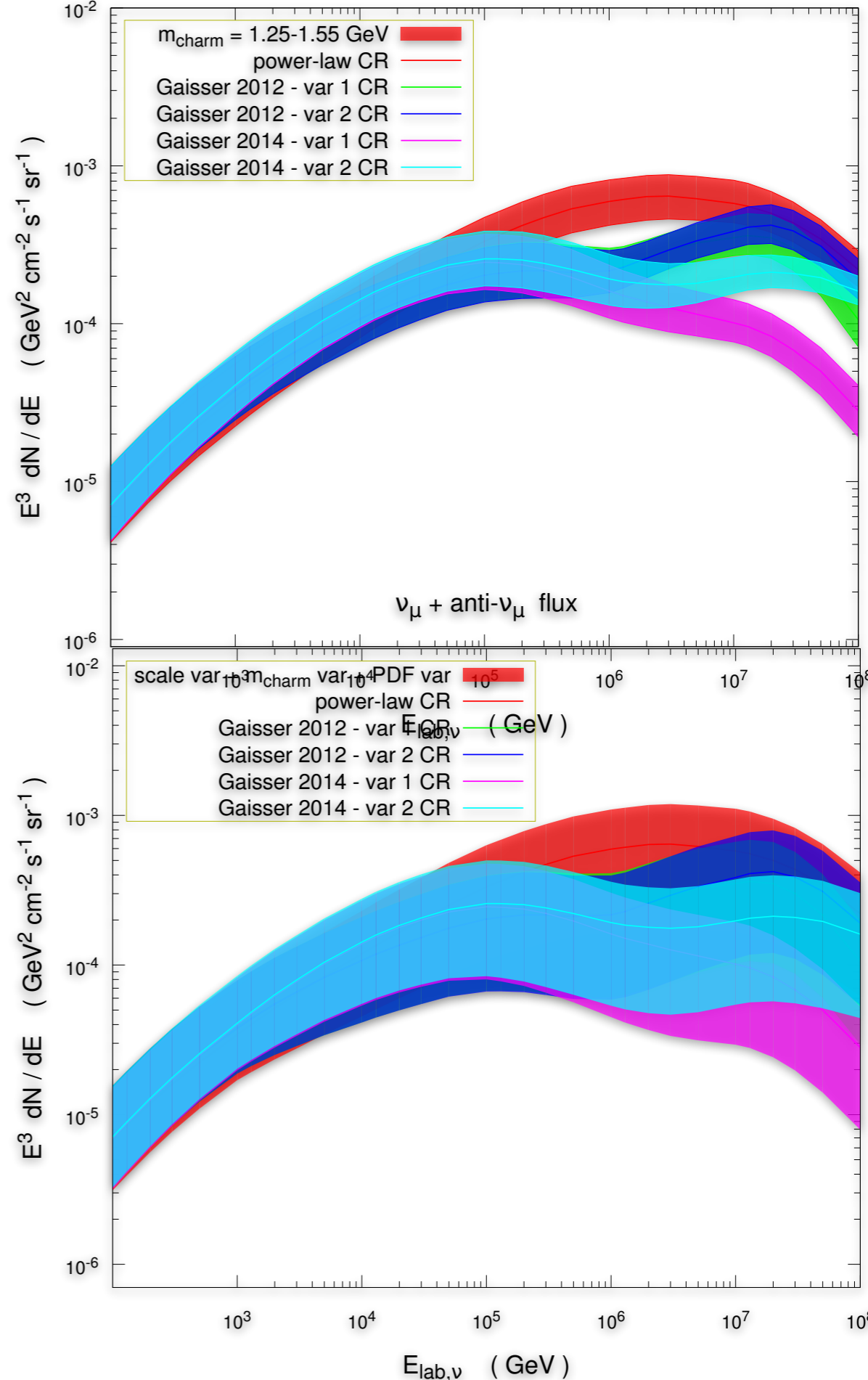
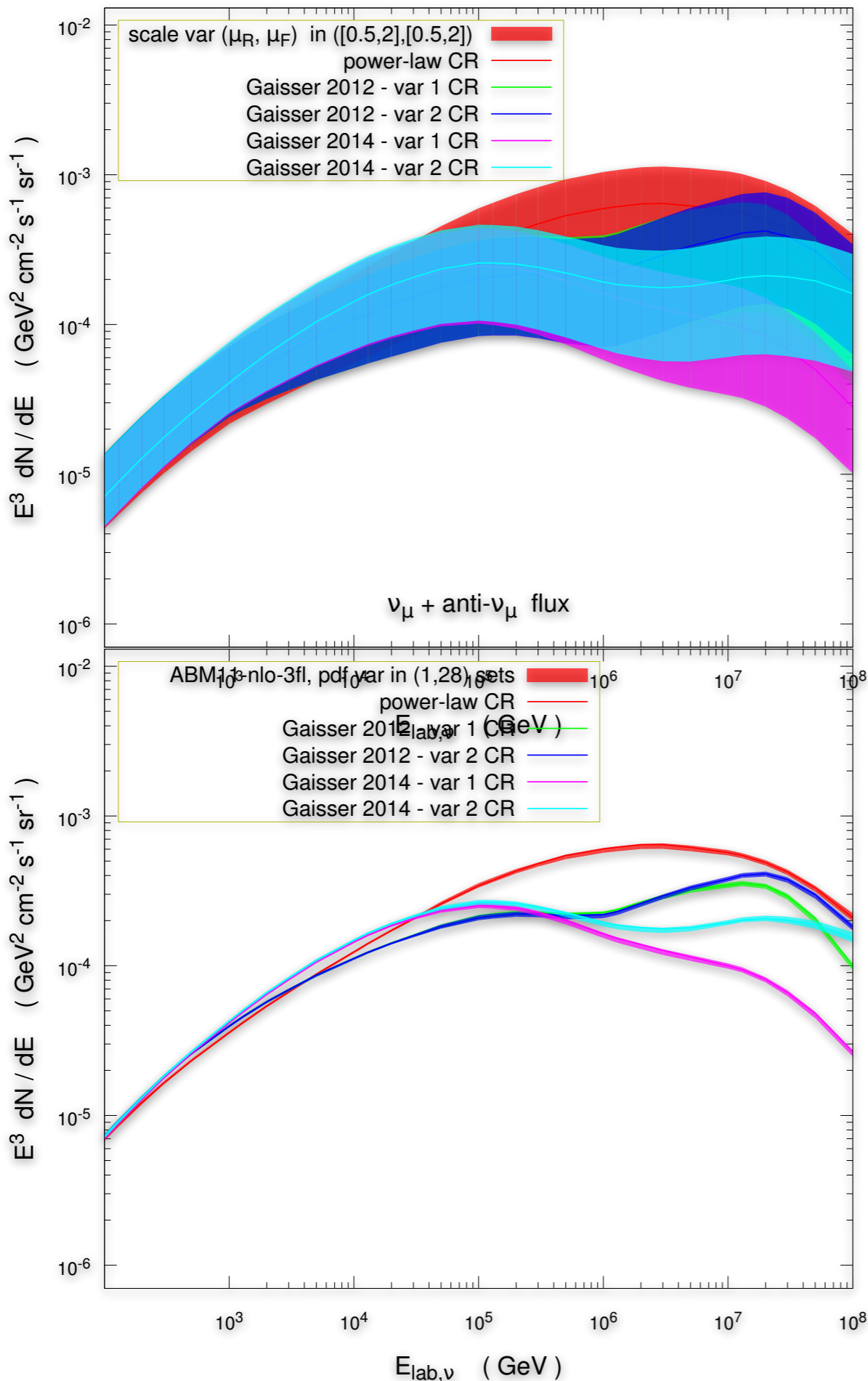
PDF variation

 $\nu_\mu + \text{anti-}\nu_\mu$ flux $\nu_\mu + \text{anti-}\nu_\mu$ flux

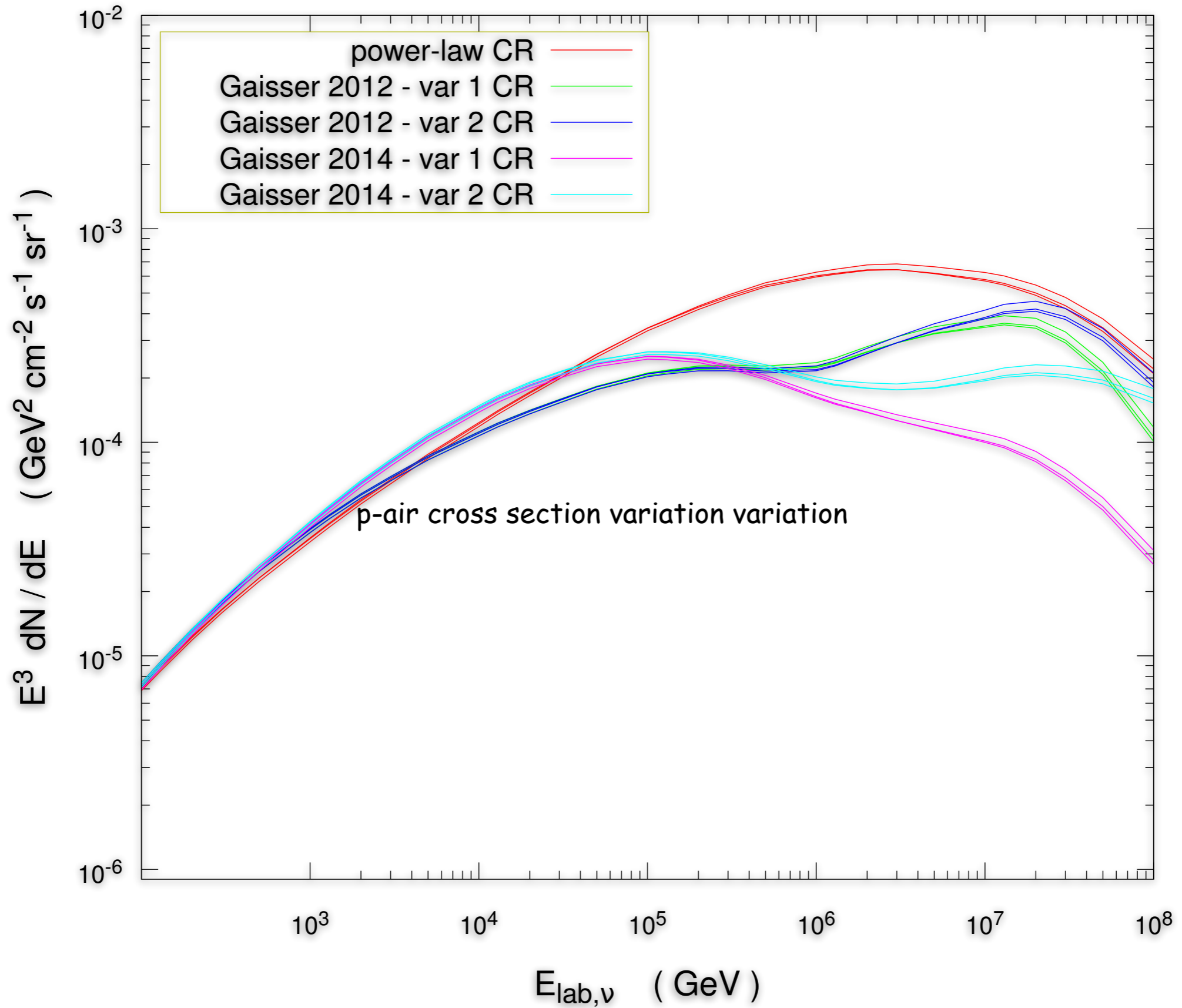
Summary of variations

$\nu_\mu + \text{anti-}\nu_\mu$ flux

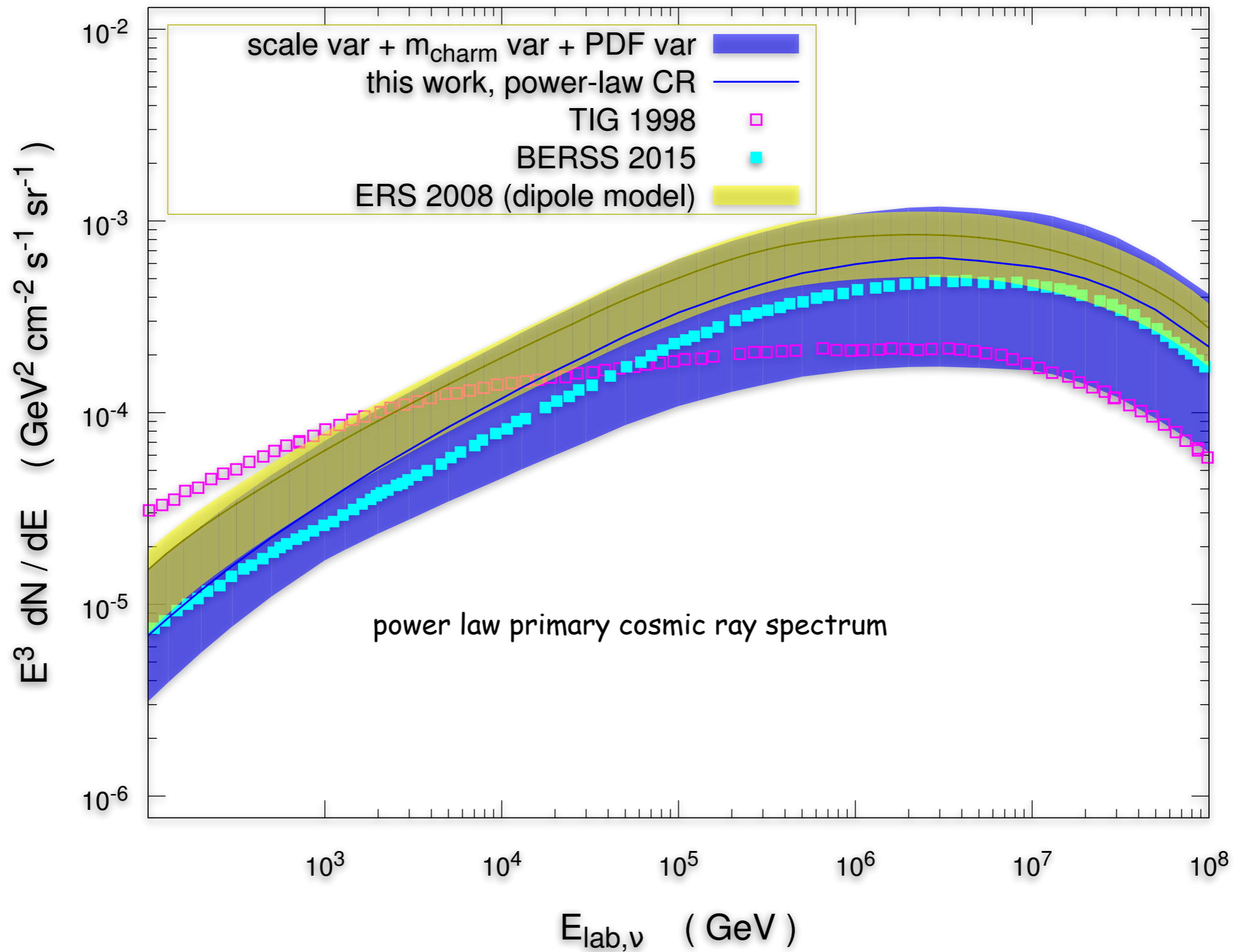
$\nu_\mu + \text{anti-}\nu_\mu$ flux

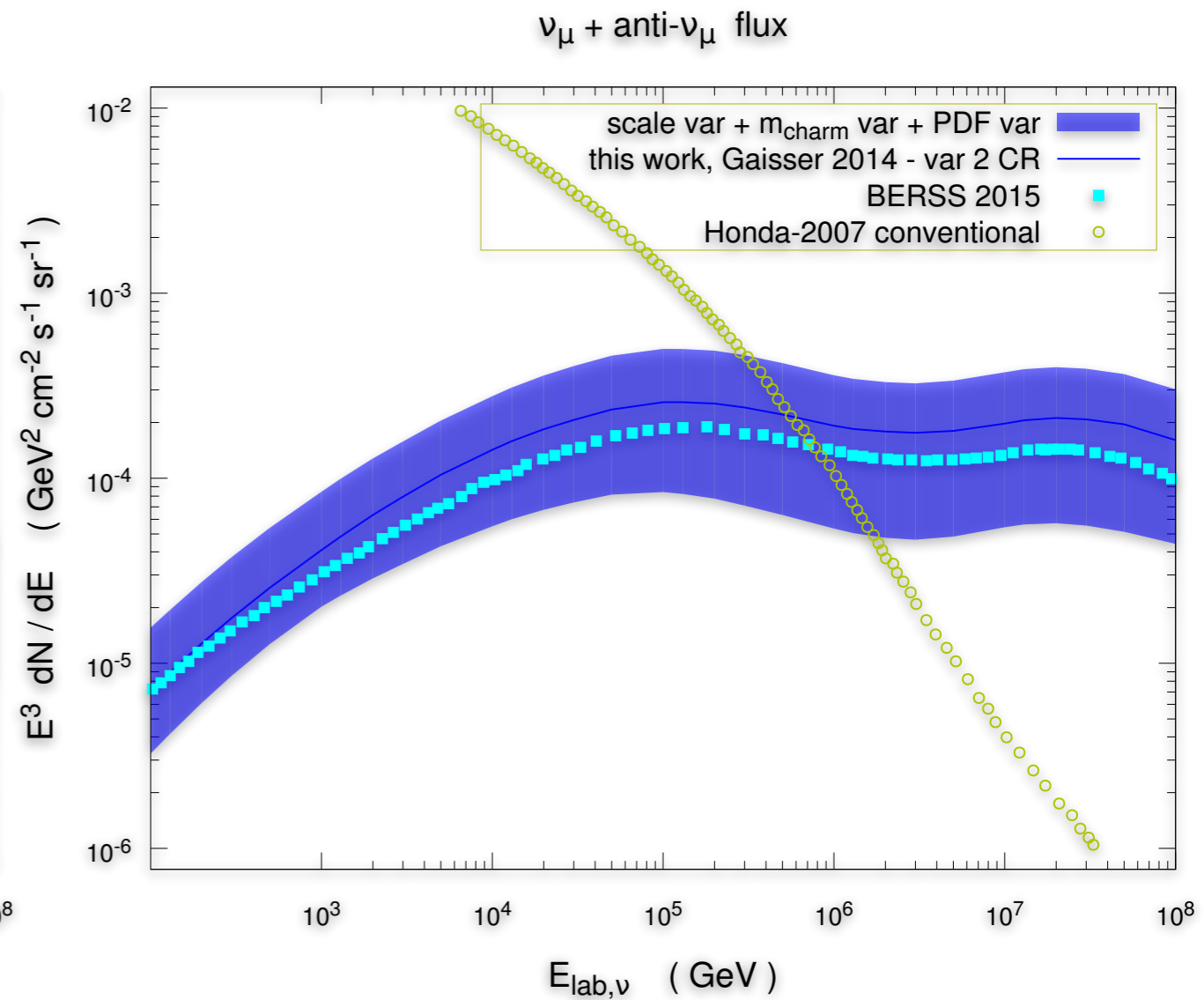
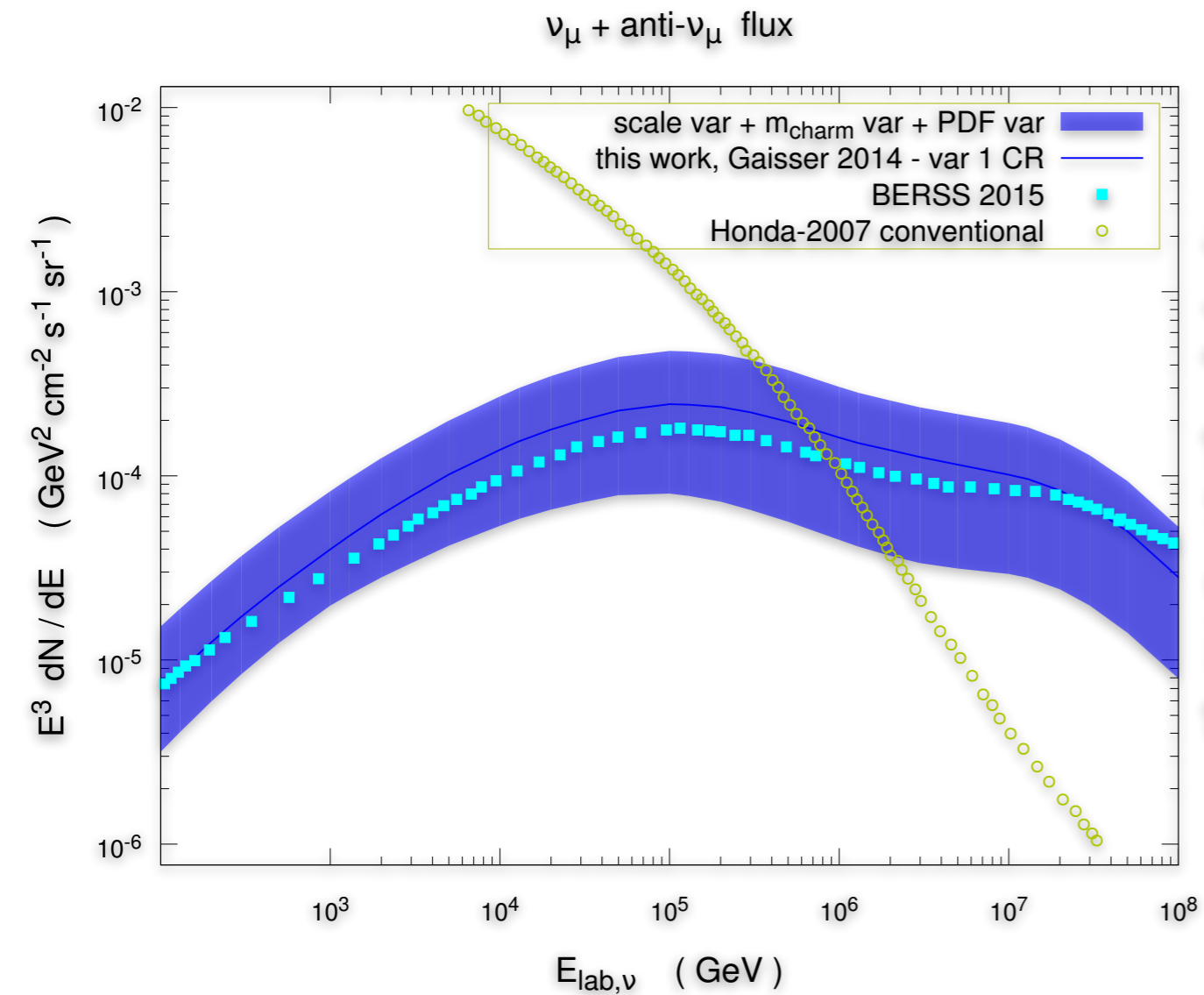


$\nu_\mu + \text{anti-}\nu_\mu$ flux



$\nu_\mu + \text{anti-}\nu_\mu$ flux

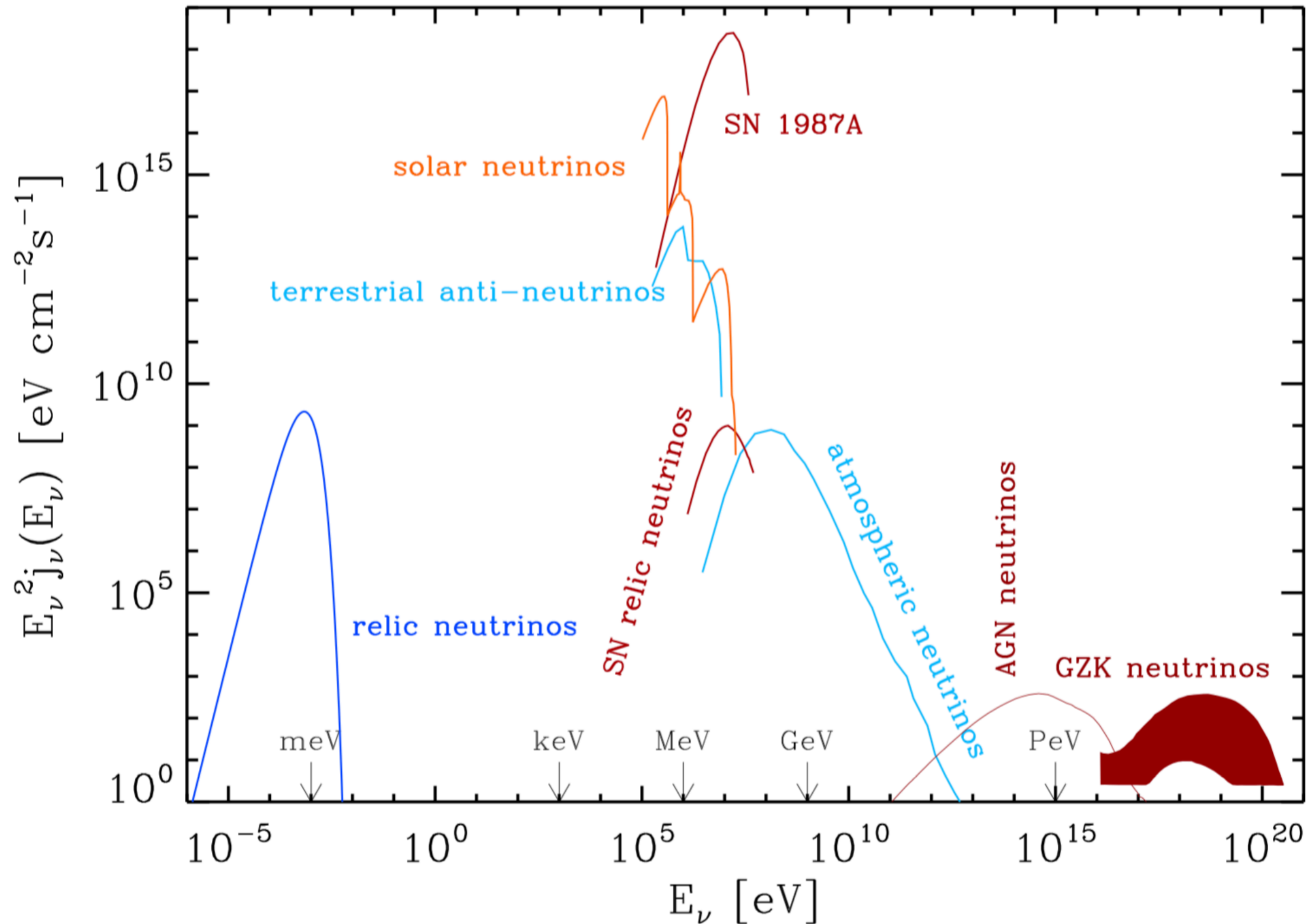




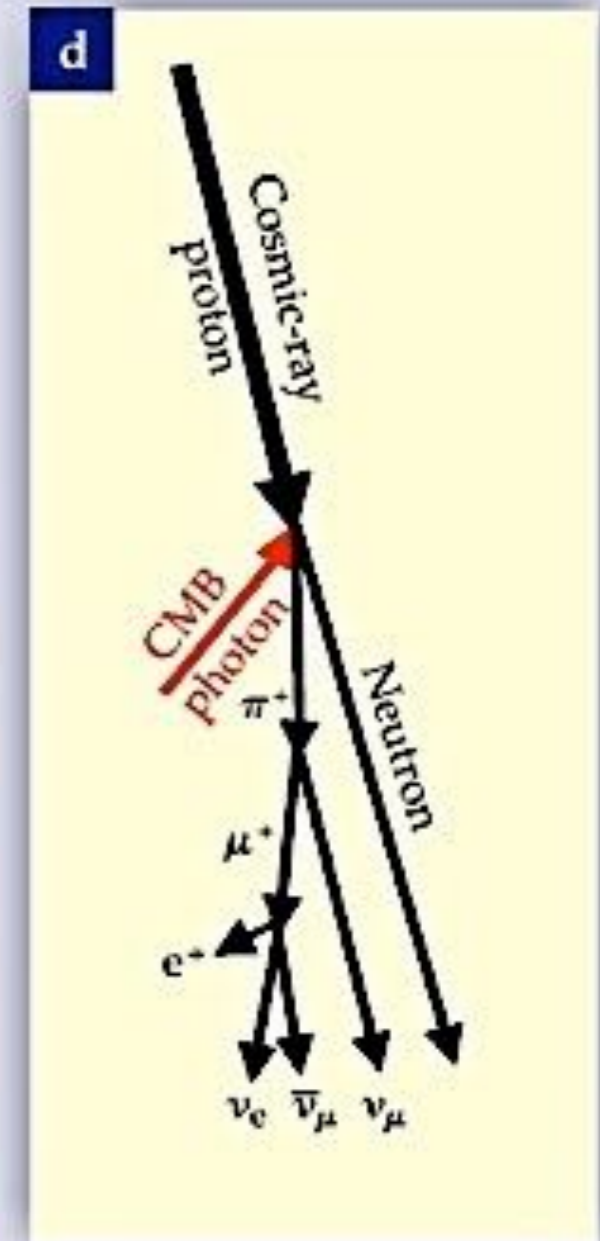
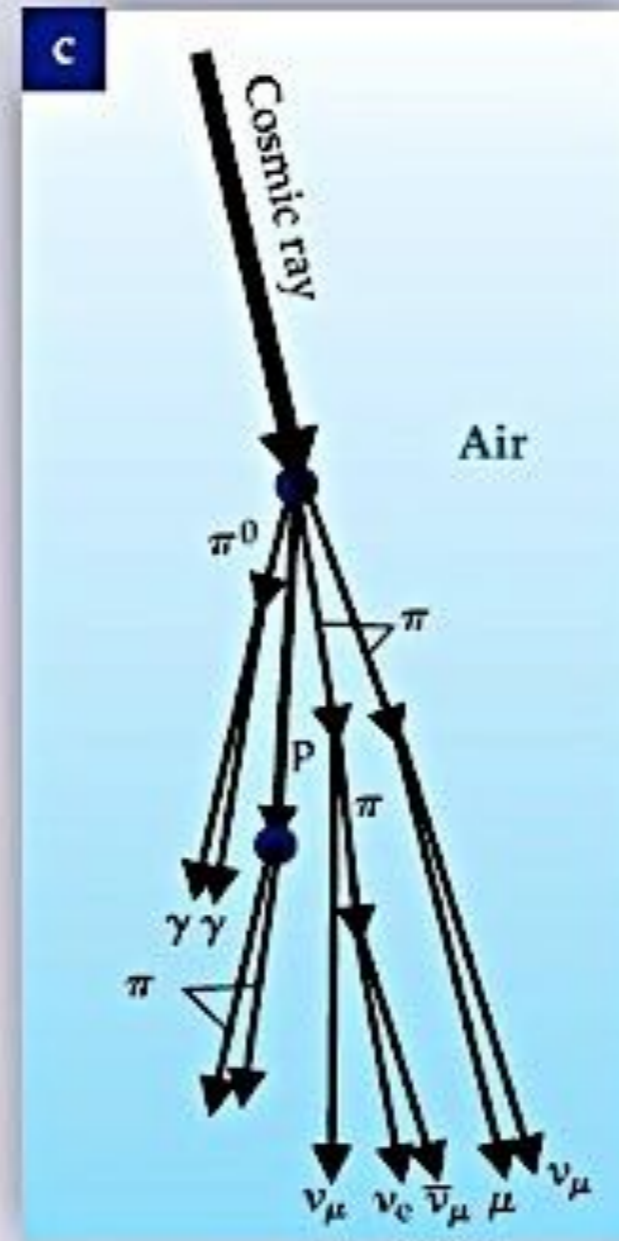
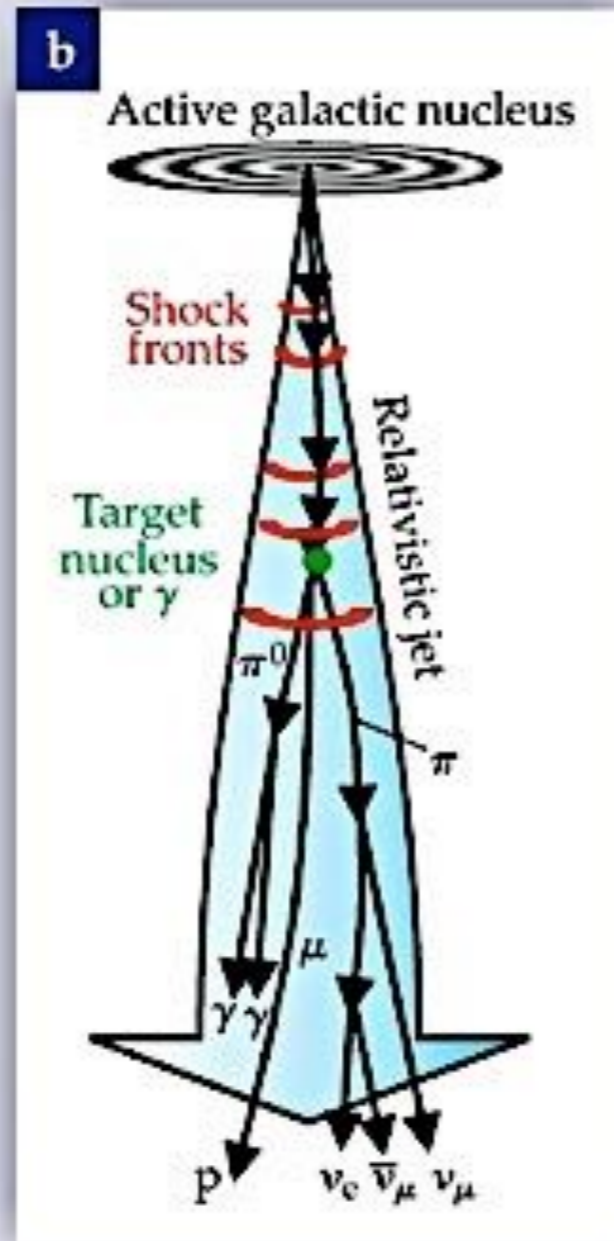
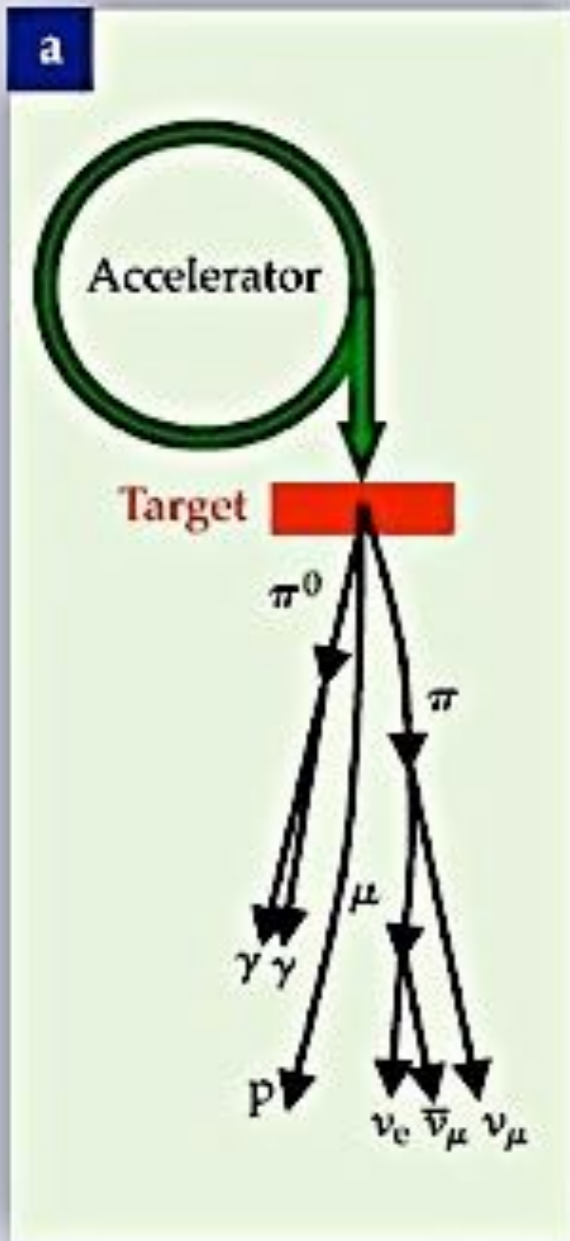
extragalactic mixed (left panel) versus pure proton (right panel) composition, Gaisser 2014

Very High High Energy Neutrinos

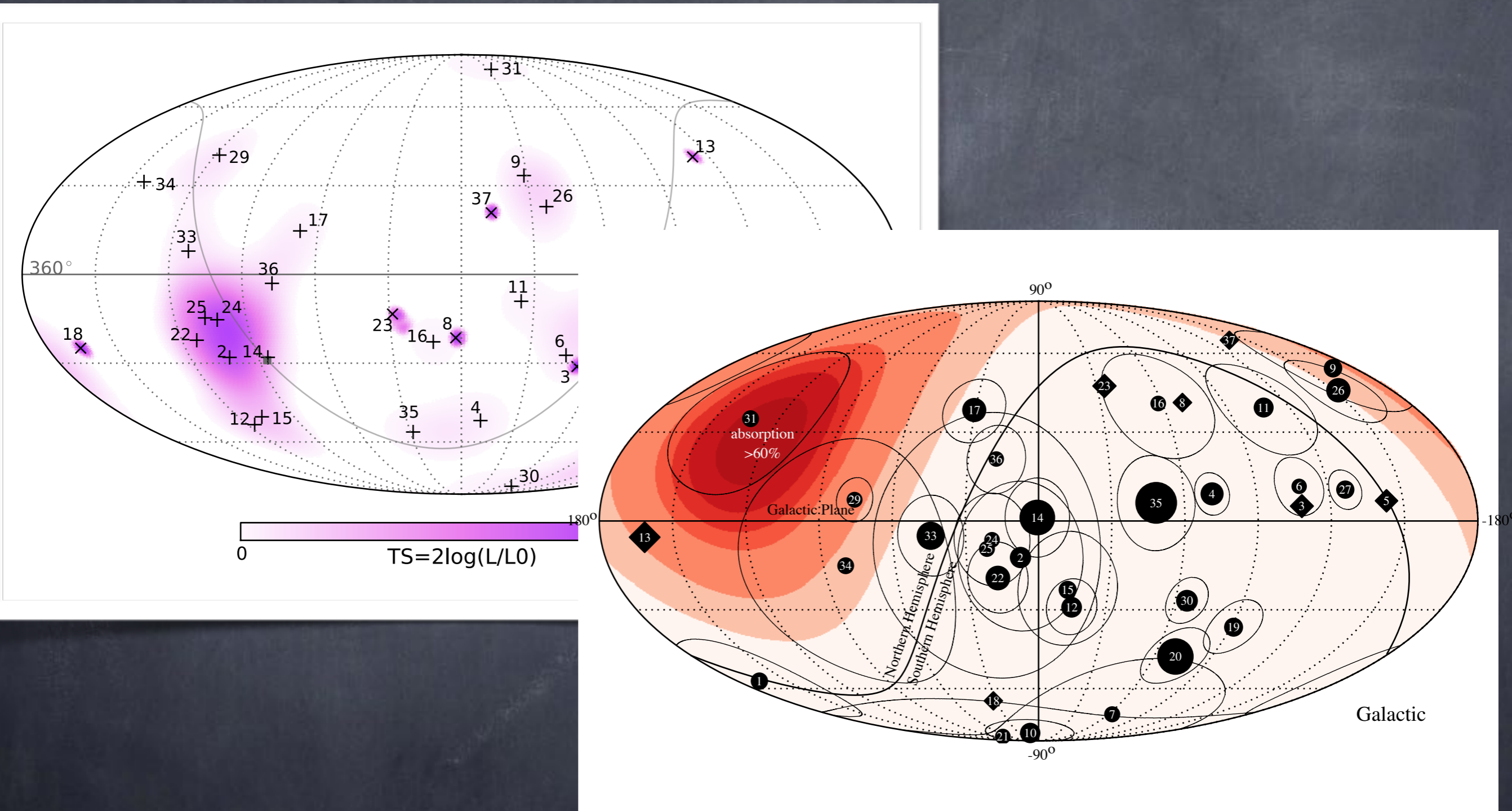
The „grand unified“ differential neutrino energy spectrum



Summary of neutrino production modes



Neutrino sky distribution

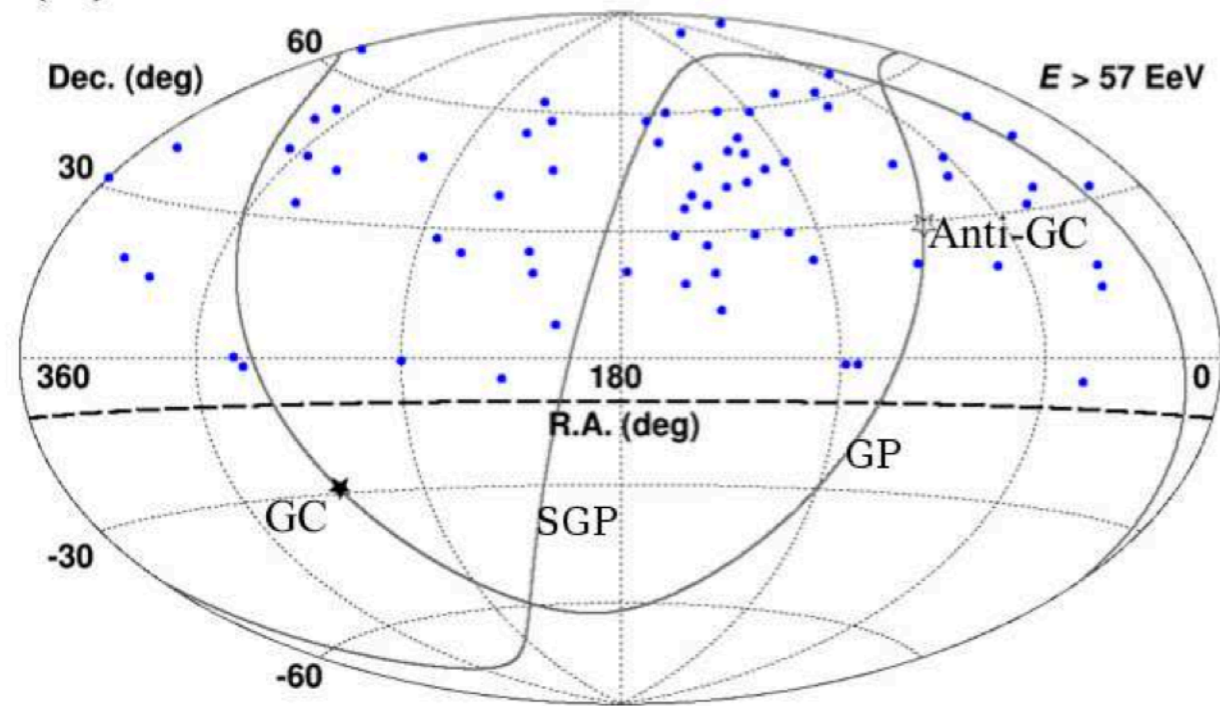


IceCube collaboration, Phys.Rev. Lett. 113 (2014) 101101 [arXiv:1405.5303]

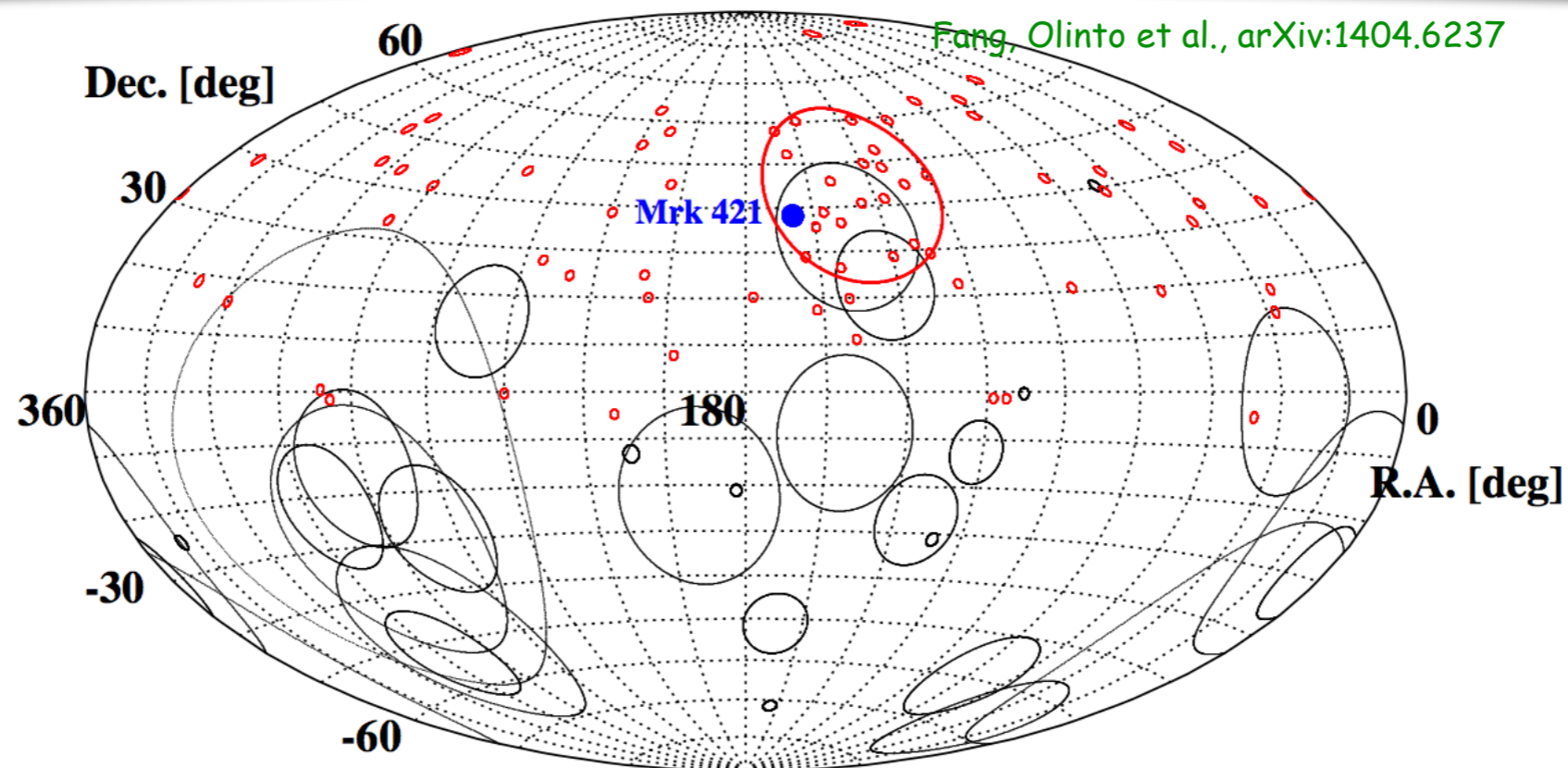
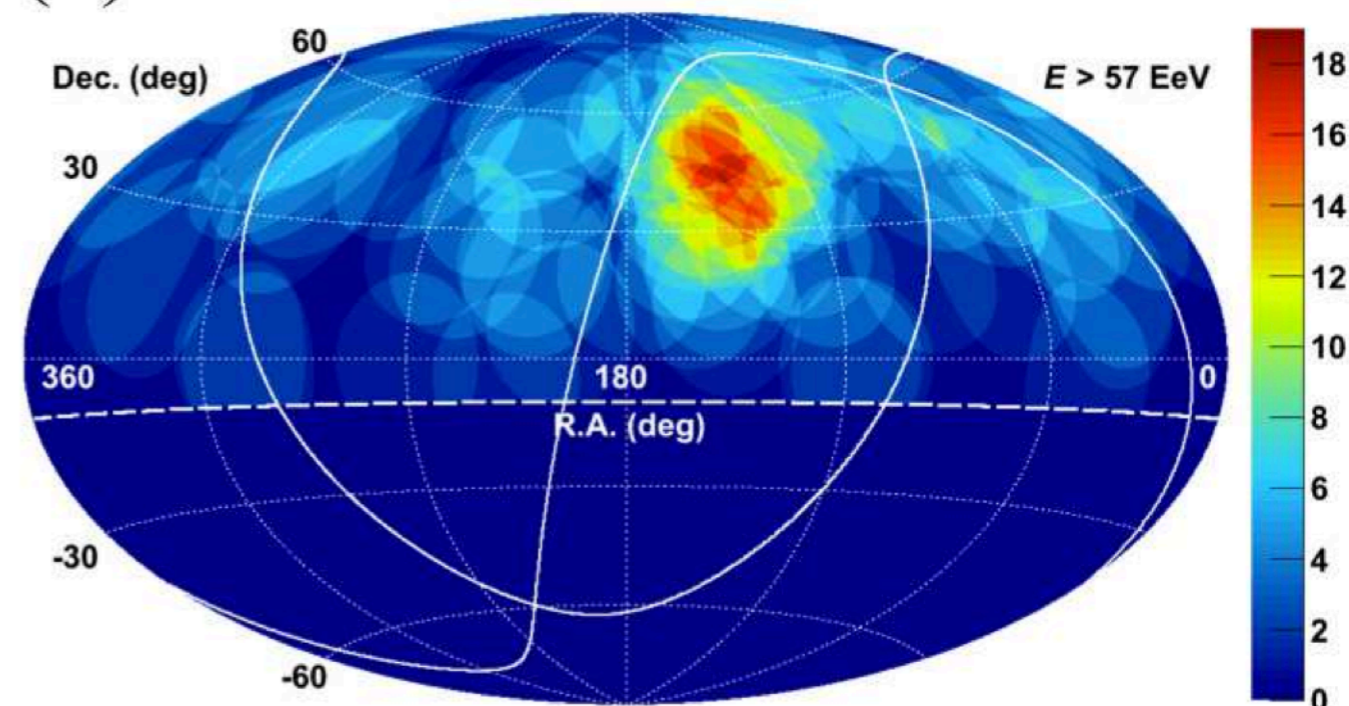
A possible Correlation of IceCube Neutrinos with the Cosmic Ray Excess seen by Telescope Array ?

Telescope Array Collaboration, ApJ. Lett. 790 (2014) L21 [arXiv:1404.5890]

(a)

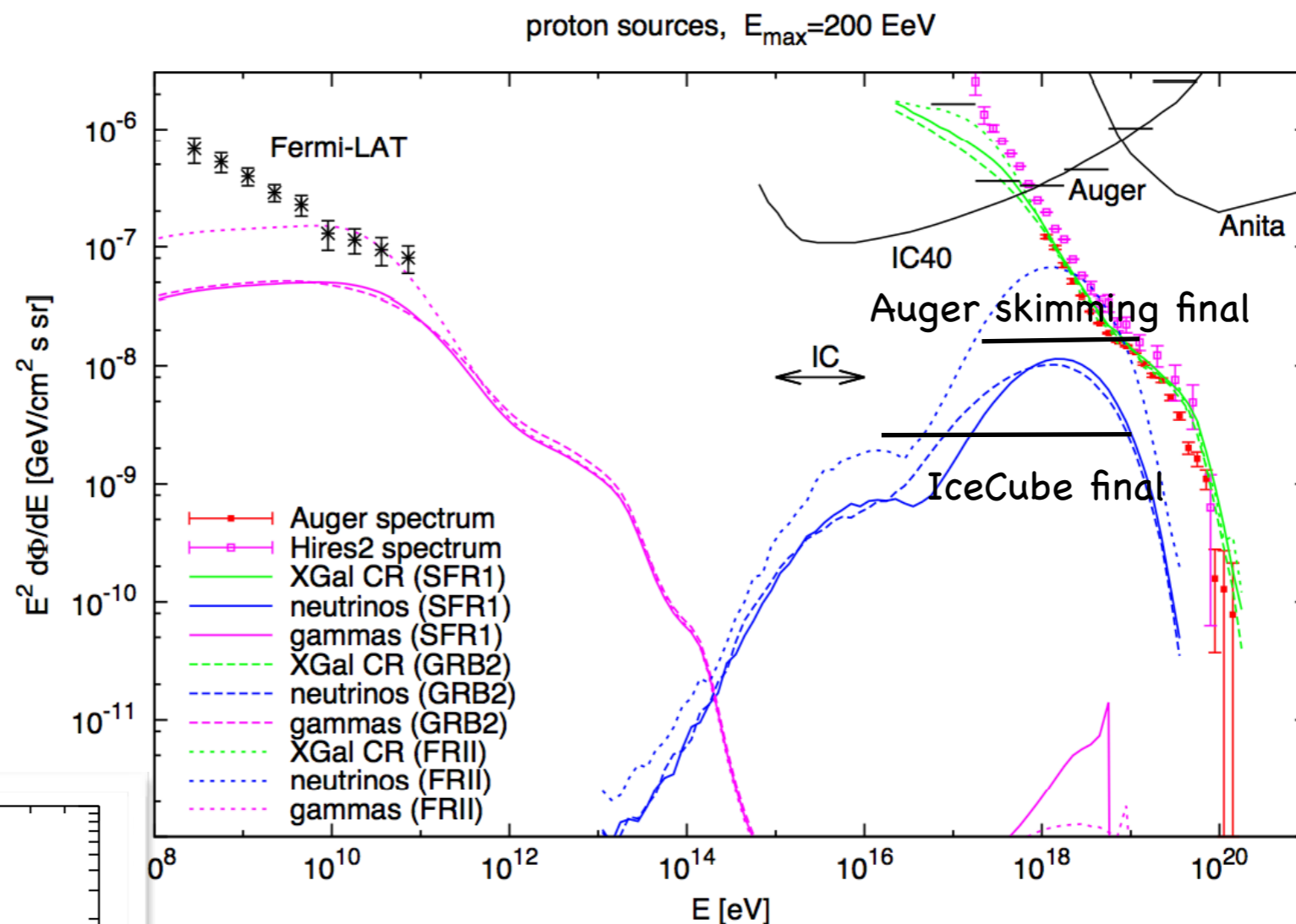
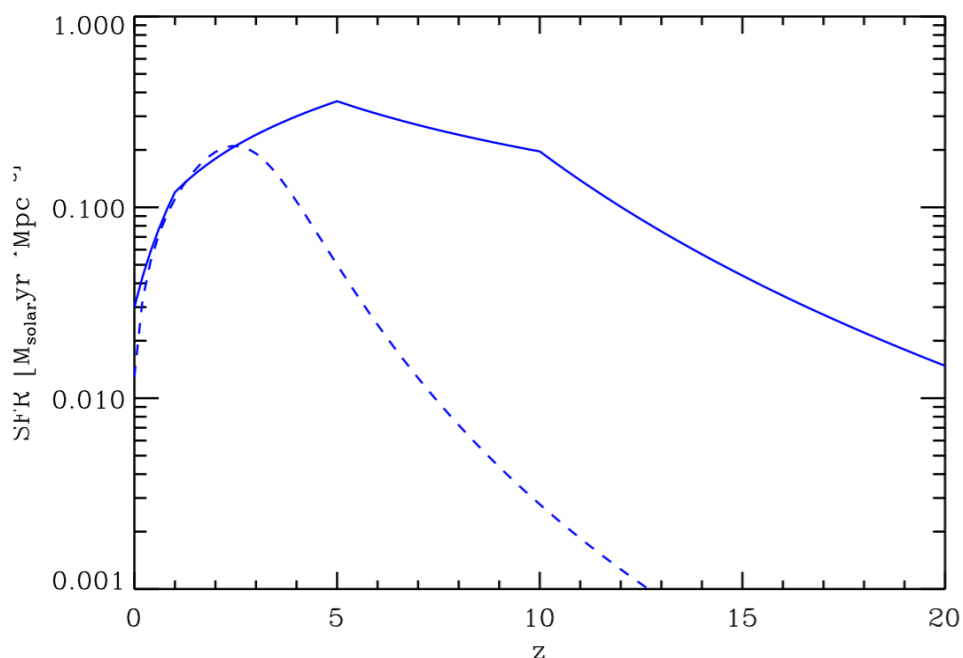


(b)

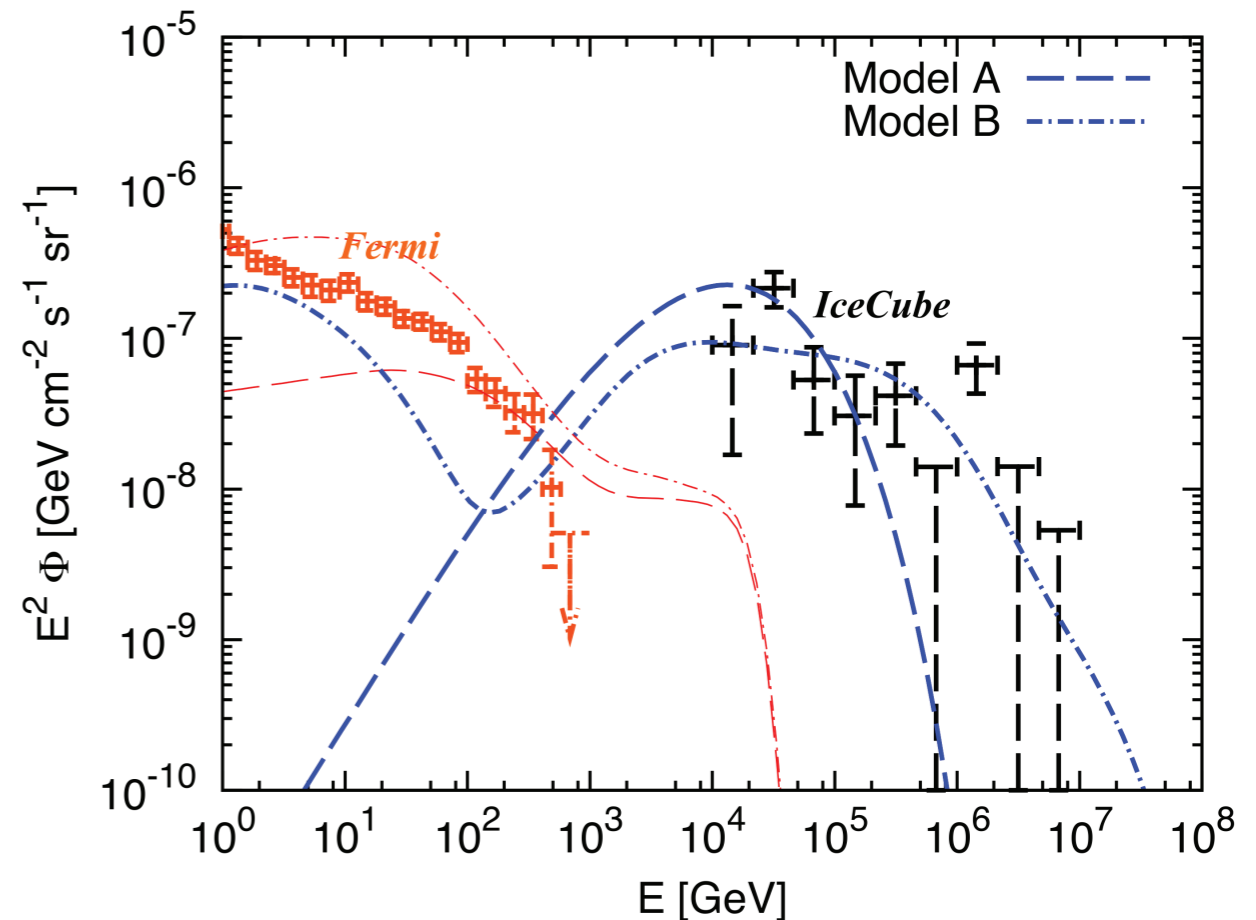
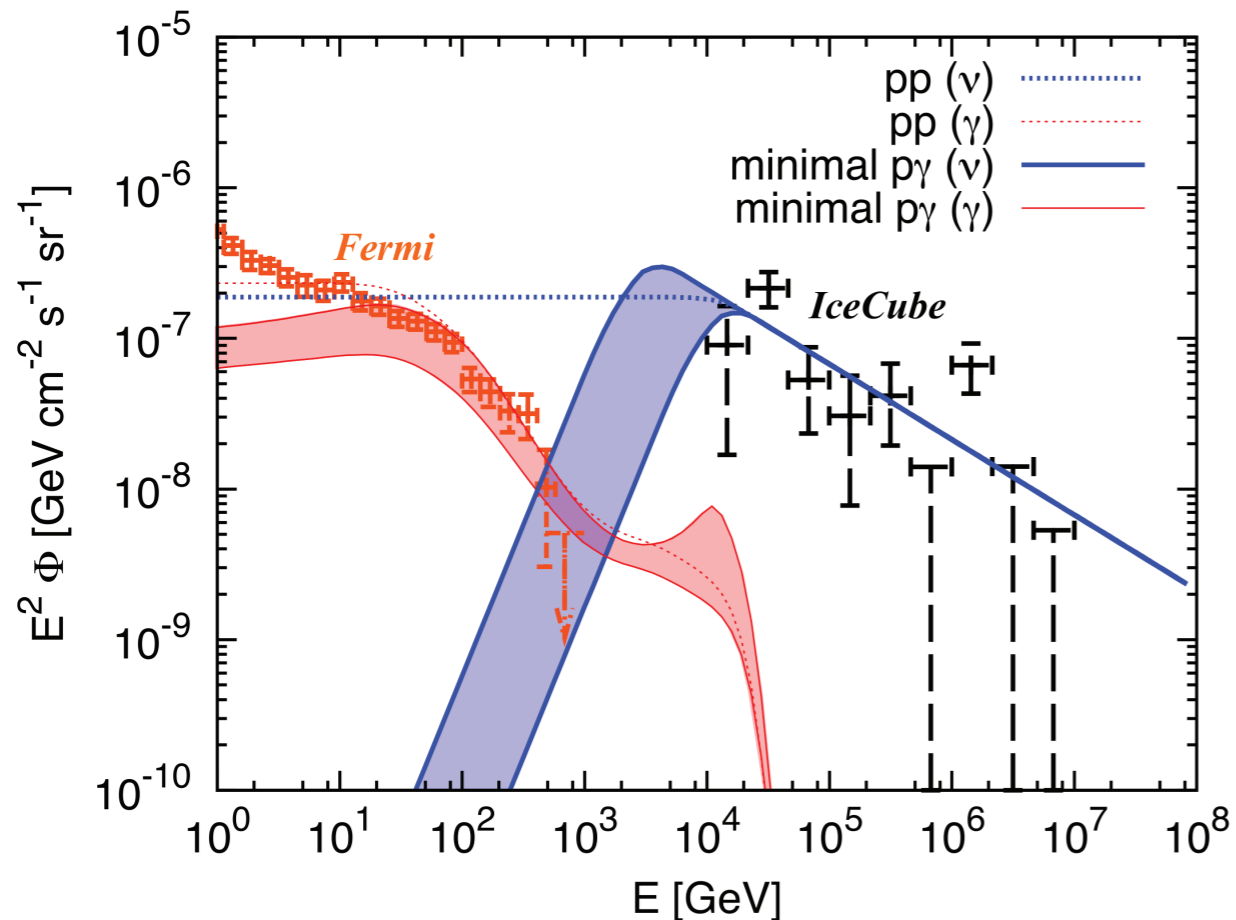


Cosmogenic Neutrinos: Maximal Fluxes for Pure Proton Injection insufficient to explain IceCube neutrinos

- Including secondary photons
- strong source evolution is here constrained by Fermi-LAT results



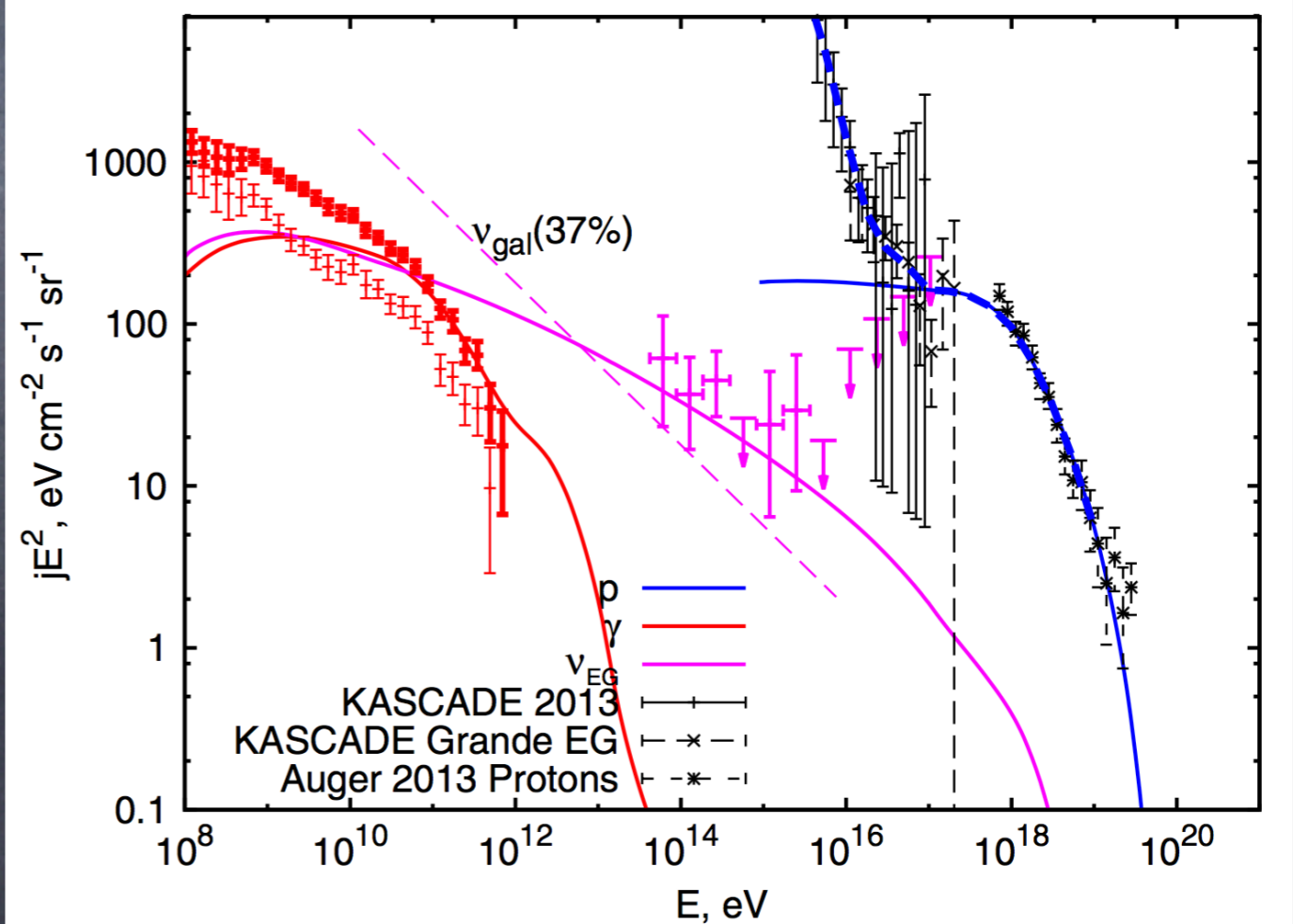
In scenario with $E_{\max} = 200$ EeV for different source evolution models (SFR1, GRB2) source spectral index is $\alpha = 2.4$ for the SFR1 and GRB2 models, while $\alpha = 2.2$ for FR11. Indicated are the propagated proton spectrum, the resulting (all flavor) neutrino fluxes. The photon background measured by Fermi-LAT [10] is indicated, besides the ν bounds included in figure 1.



Murase, Guetta, Ahlers, PRL 116}, 071101 (2016)

Sources may have to be "hidden" in gamma-rays and primary cosmic rays to be consistent with other data

Giacinti, Kachelrieß, Kalashev, Neronov, Semikoz, PRD 92}, 083016 (2015)



Effective Penetration Depth of Electromagnetic Cascades

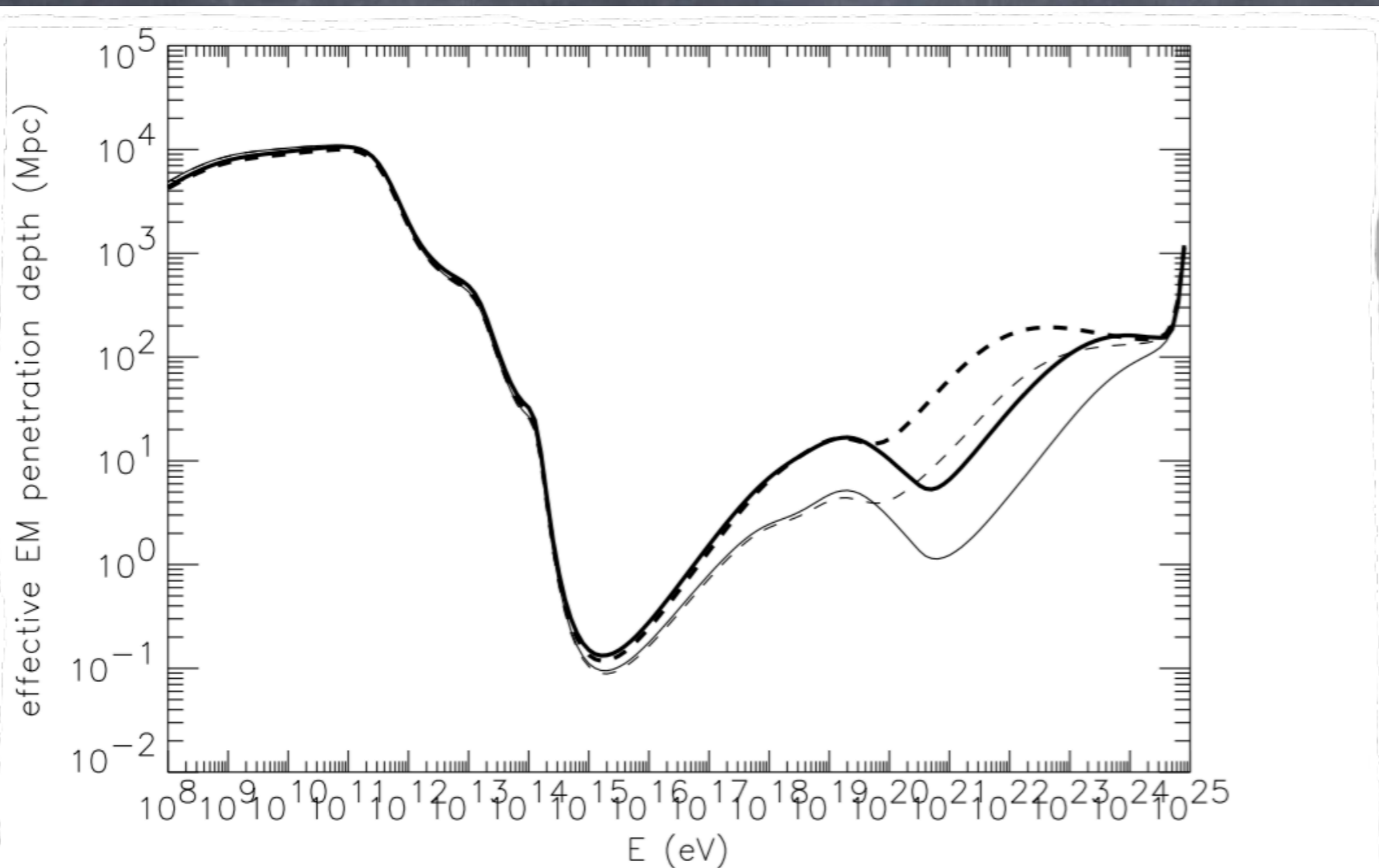
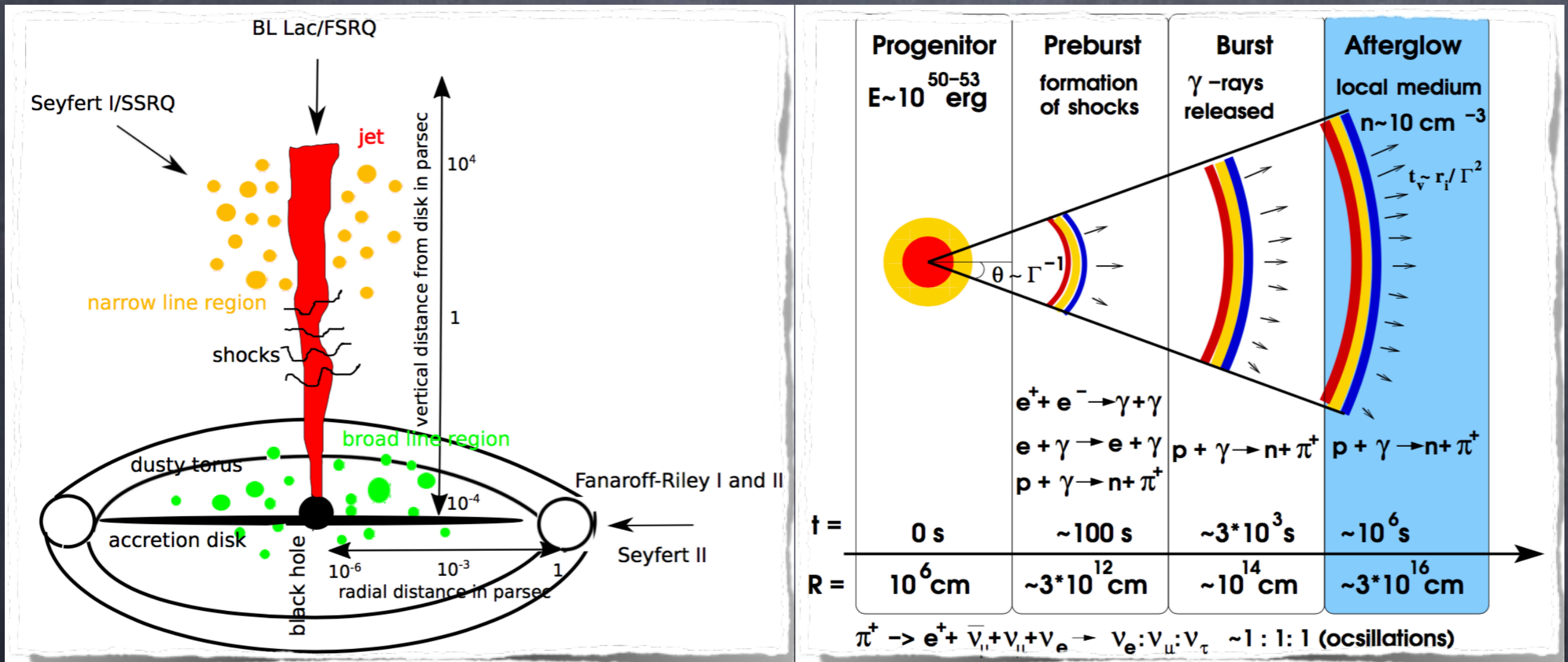


Fig. 8.6 Effective **penetration** depth of EM cascades, as defined in the text and its dependence on uncertainties of the universal radio background, see the red band at low energies in Fig. 5.16, and the EGMF. Solid lines are for a strong universal radio background estimate, dashed lines for a lower estimate for this background, and thick lines correspond to an EGMF $\ll 10^{-11}$ G whereas thin lines are for 10^{-9} G, respectively. Reprinted figure from Ref. [157], P. Bhattacharjee and G. Sigl, Phys. Rept. **327**, 109 (2000), [http://dx.doi.org/doi:10.1016/S0370-1573\(99\)00101-5](http://dx.doi.org/doi:10.1016/S0370-1573(99)00101-5), with permission from Elsevier.

Discrete Extragalactic High Energy Neutrino Sources

IceCube neutrinos should be produced mostly within sources, not during propagation

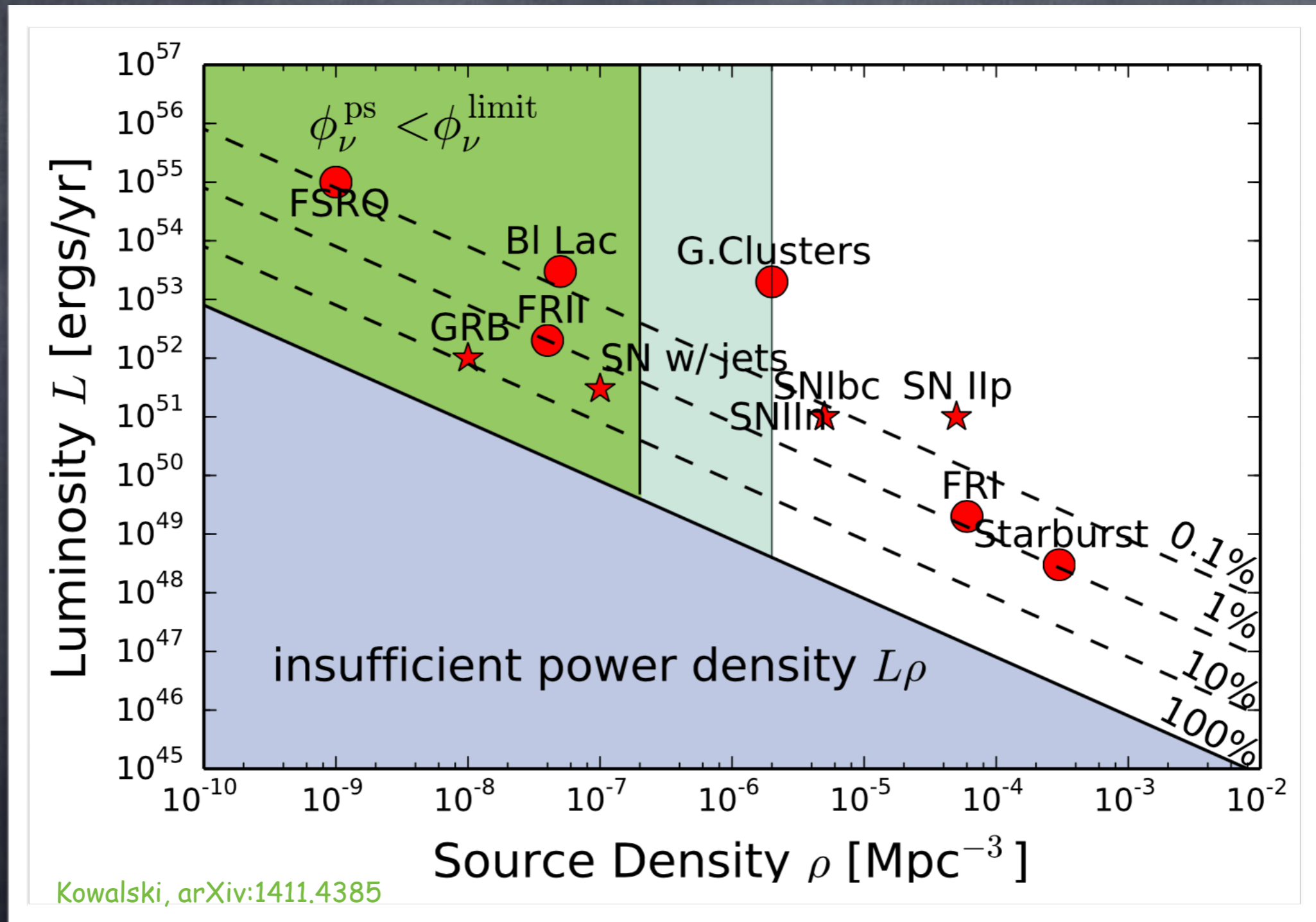


active galaxies

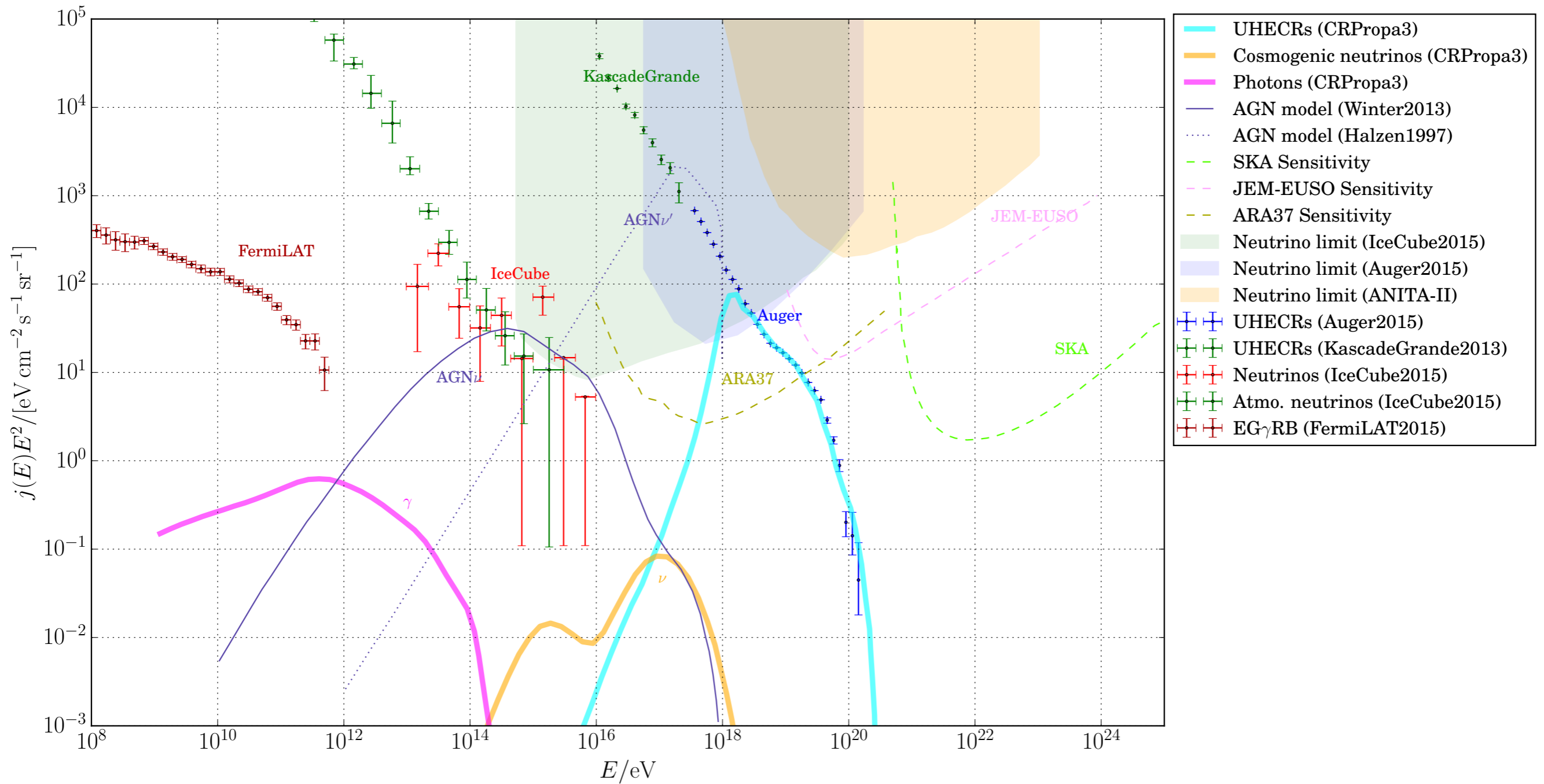
gamma ray bursts

Figures adapted from J. Becker-Tjus, Phys.Rep. 458 (2008) 173

But a combination of the measured diffuse flux with upper limits on individual sources constrains source type



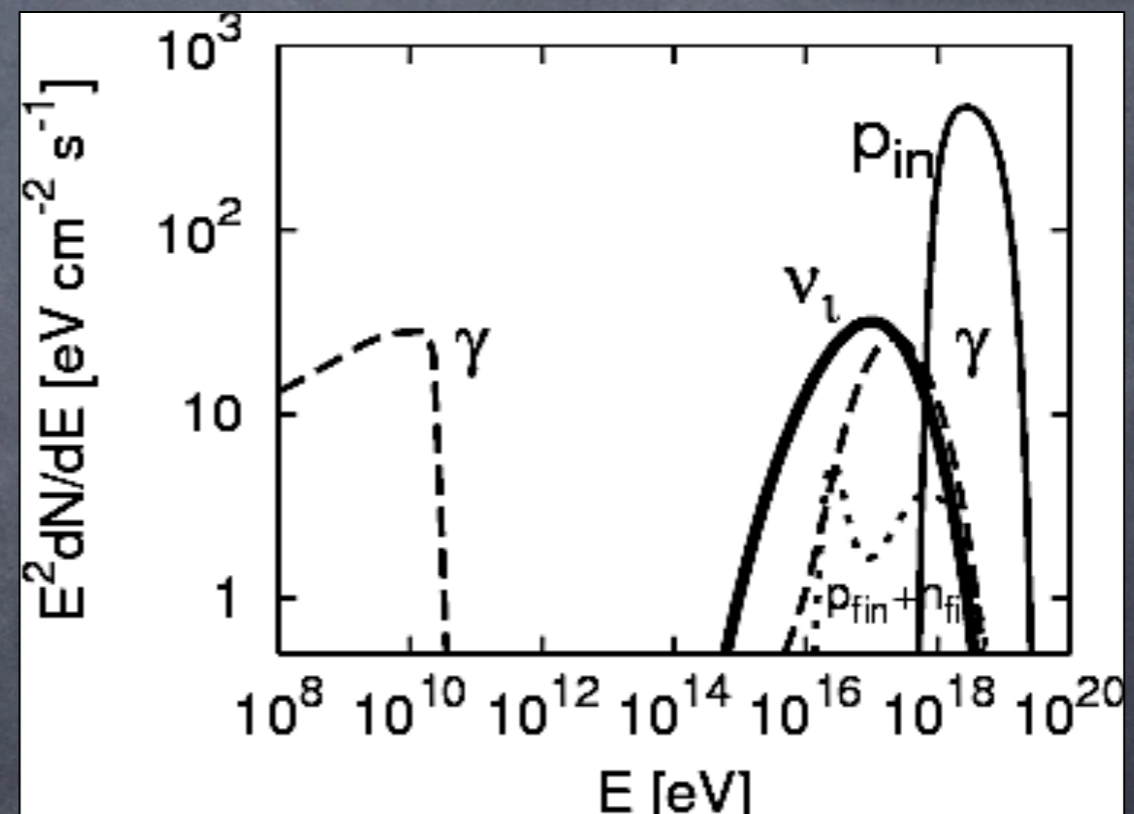
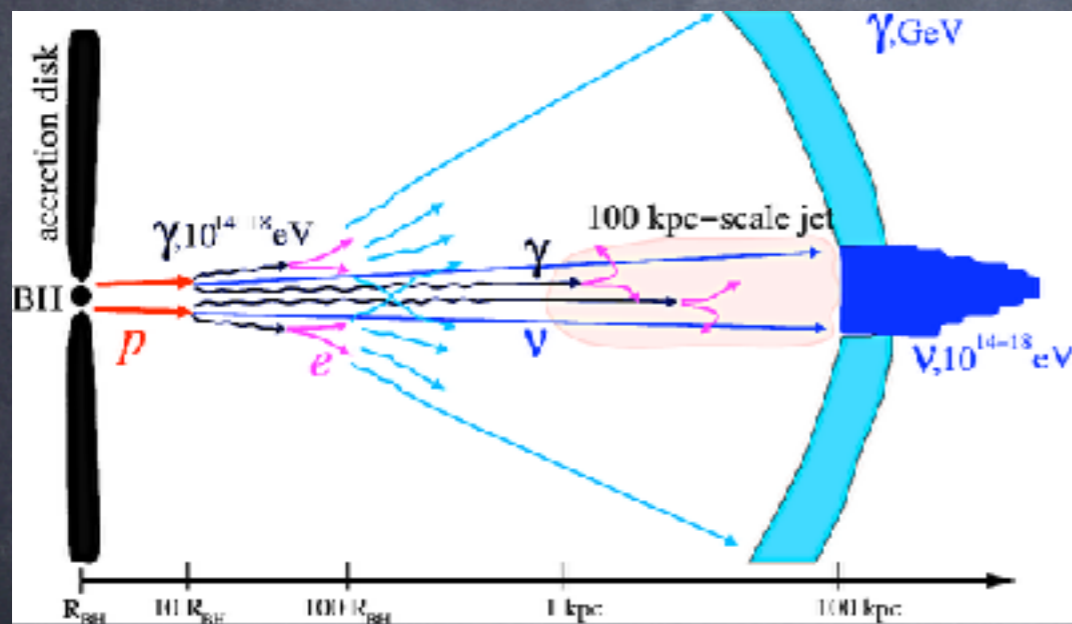
Multi-Messengers: The Big Picture



General Multi-Messenger Aspects

Blazars emitting significant neutrino sources should be loud in GeV γ -rays, but NOT in γ -rays above TeV.

This is because such γ -rays pair produce with "blue bump" photons of ~ 10 eV energy with a cross section $\sim \sigma_{\text{Th}} \sim 1$ b about a factor 10^4 larger than the $p\gamma$ cross section that produces the neutrinos \Rightarrow If loud in $> \text{TeV}$ γ -rays, optical depth for neutrino production would be very small.



Neronov and Semikoz, Phys.Rev.D66 (2002) 123003

Conclusions

- 1.) Our atmospheric charm component of muon neutron flux is about 40% higher than previous calculations
- 2.) more importantly, uncertainties are relatively large, up to a factor ten; dominated by QCD up to $\sim 10^5$ GeV and by cosmic ray total nucleon flux at higher energies
influence of composition (and flux) uncertainties should be updated and projected as a band
- 3.) Atmospheric neutrinos are an important background for astrophysical neutrinos for which model and constraint building is now in full gear